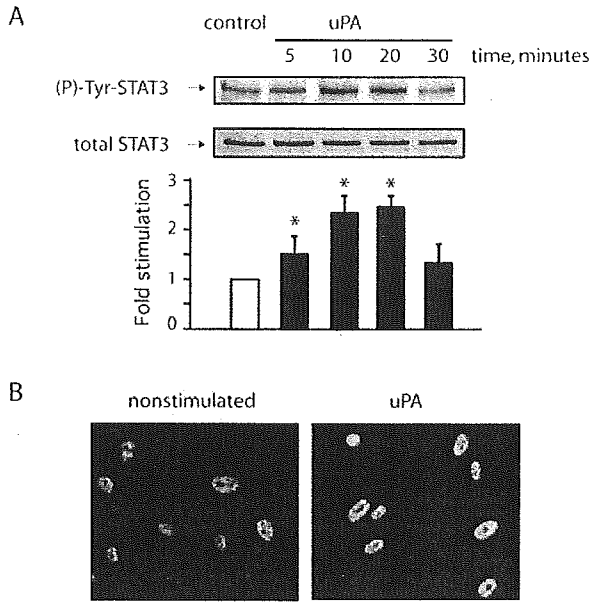

Fig. 4. uPA induces activation and nuclear translocation of Stat3 in MCs. (A) Quiescent MCs were treated with 10 nM uPA for the indicated times and phosphorylated Stat3 protein was visualized in cell lysates by immunoblotting with specific anti-(P)-Tyr-Stat3 antibodies. MCs incubated in medium without uPA served as a control. The middle panel demonstrates the amount of total Stat3 loaded on the gel for each sample. Results are representative of three independent experiments. Quantification (mean ± s.e.m.) of the results of these experiments by densitometry is shown below. Significance between control unstimulated and stimulated cells was determined by Student's *t*-test (**P*<0.05). (B) A subconfluent MC monolayer was treated with 10 nM uPA at 37°C or left untreated, fixed and stained using primary anti-(P)-Tyr-Stat3 antibody and the corresponding Alexa Fluor-488 secondary antibody. The data are representative of three separate and independent experiment performed in duplicate for each condition.

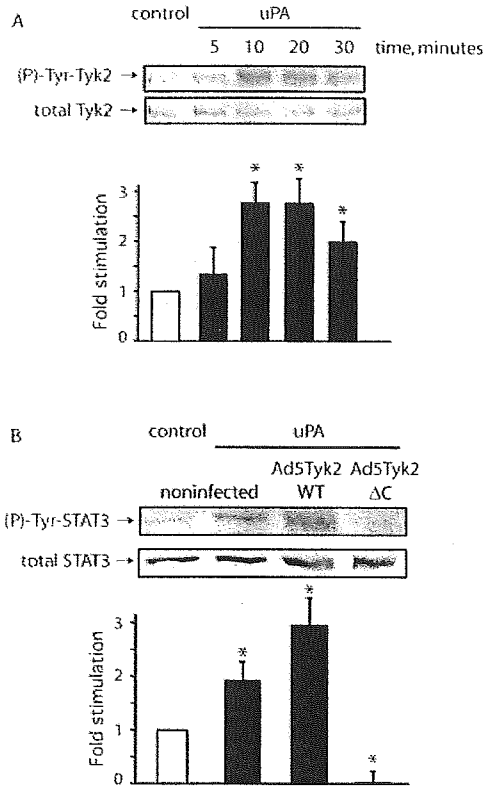

Fig. 5. uPA induces activation of Tyk2 in MCs. (A) Quiescent MCs were treated with 20 nM uPA for the indicated times and phosphorylated Tyk2 protein was visualized in cell lysates by immunoblotting with specific anti-phospho-Tyk2 antibodies (upper panel). MCs incubated in medium without uPA served as a control. The middle panel demonstrates the amount of total Tyk2 loaded on the gel for each sample. Results are representative of three independent experiments. Quantification (mean ± s.e.m.) of the results for these experiments by densitometry is shown below. Significance between control unstimulated and stimulated cells was determined by Student's *t*-test (**P*<0.05). (B) MCs were left uninfected or were infected with wild-type Ad5Tyk2 or with the mutant form, Ad5Tyk2ΔC, and then stimulated for 20 minutes with 20 nM uPA. Phosphorylated Stat3 protein was visualized in cell lysates by immunoblotting with specific anti-(P)-Tyr-Stat3 antibodies. Noninfected MCs incubated in medium without uPA served as a control. The middle panel demonstrates the equal amount of total Stat3 loaded on the gel for each sample. Results are representative of three independent experiments. Quantification (mean ± s.e.m.) of the results by densitometry is shown for three experiments is shown below. Significance between control unstimulated and stimulated cells was determined by Student's *t*-test (**P*<0.05).

expressed in MCs. As shown in Fig. 5B, uPA-induced Stat3 activation was completely abrogated in Ad5Tyk2ΔC-expressing MCs, as compared to non-infected and wild-type Ad5Tyk2-expressing cells. We conclude from these results that Tyk2 is required for the activation of Stat3 by uPA in MCs.

To examine the specific role of uPAR in propagation of the revealed Tyk2/Stat3 signaling, MCs with downregulated uPAR expression were used. Stable and specific inhibition of uPAR expression was achieved using a lentiviral RNA interference vector LV-uPARsi (Fig. 6A). Neither Tyk2 nor Stat3 phosphorylation was observed in LV-uPARsi-MCs, in contrast to cells infected with control vector (Fig. 6B,C).

Tyk2/Stat3 pathway mediates C5aR expression in MCs in response to uPA

To evaluate the role of the Tyk2/Stat3 pathway in the uPA-directed control of C5aR expression, several experiments were performed. MCs transiently infected with wild-type Ad5Tyk2 and two mutant forms, Ad5Tyk2KE and Ad5Tyk2ΔC, were stimulated with uPA, and C5aR expression was monitored by TaqMan analysis. Whereas there was a strong increase in C5aR mRNA in non-infected and in Ad5Tyk2-infected cells, Ad5Tyk2KE- and Ad5Tyk2ΔC-expressing cells did not respond to uPA stimulation. Consistent with these data, no uPA-induced stimulation in C5aR expression was observed in MCs expressing the Stat3F mutant form of Stat3 (Fig. 7). These results assign a direct role to the Tyk2/Stat3 pathway in controlling immune competent receptors response to uPA.

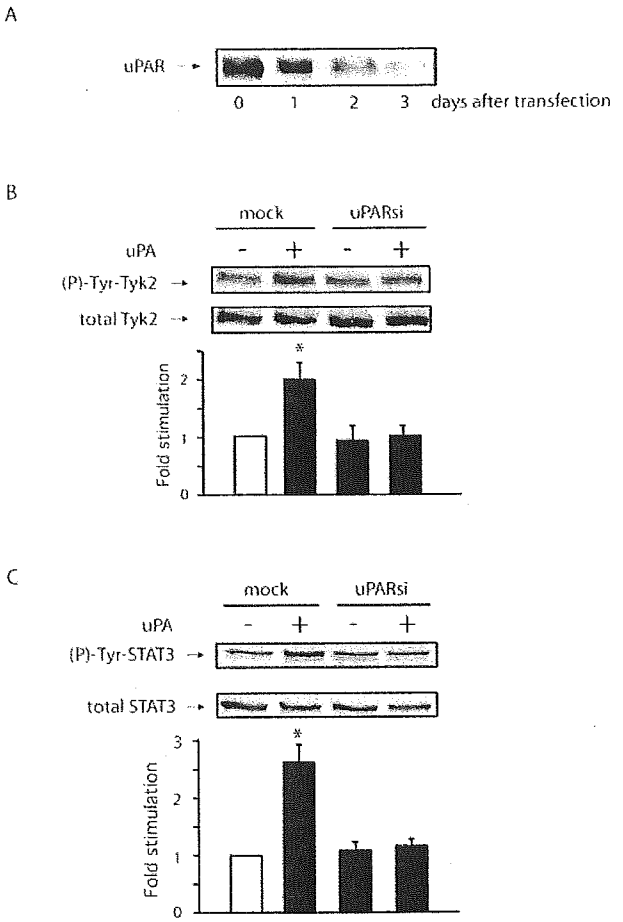

Fig. 6. uPAR mediates uPA-dependent Tyk2/Stat3 pathway activation in MCs. A. Quiescent MCs were infected with LV-uPARsi and time-dependent downregulation of uPAR expression was monitored by immunoblotting, using clone R3 monoclonal anti-uPAR antibody. MCs infected with LV-uPARsi or mock viruses were treated with 10 nM uPA for the indicated times at day 3 after infection and phosphorylated Tyk2 (B) or Stat3 (C) proteins were visualized in cell lysates by immunoblotting with specific anti-phospho-Tyk2 and anti-(P)-Tyr-Stat3 antibody, respectively. MCs incubated in medium without uPA served as a control. The upper panels is representative of three independent experiments. Quantification (mean ± s.e.m.) of the results by densitometry is shown below. Significance between control unstimulated and stimulated cells was determined by Student's *t*-test (*P<0.05).

uPAR utilizes gp130 adaptor protein to mediate C5aR expression in MCs

As uPAR is devoid of catalytic activity and linked to the outer membrane leaflet by a glycosylphosphatidylinositol (GPI) anchor, its signaling capacities and biological functions rely on interactions with other transmembrane molecules. Several proteins interacting with uPAR have been identified, such as integrins, tyrosine kinase receptors and G protein-coupled receptors. It was shown that in the human kidney epithelial tumor cell line TCL-598, uPAR associates with gp130 protein, a signal transducing subunit of the receptor complexes for the IL-6 cytokine family, to activate the Jak/Stat pathway

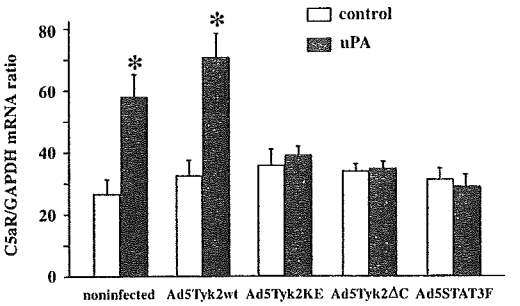

Fig. 7. TheTyk2/Stat3 pathway mediates uPA-induced upregulation of C5aR in MCs. Quiescent MCs that were uninfected or infected with wild-type Ad5Tyk2, the Tyk2 mutants, Ad5Tyk2ΔC and Ad5Tyk2KE, or with the Ad5STAT3F mutant form of Stat3 were stimulated with 20 nM uPA for 20 hours, and RT-PCR analysis for C5aR mRNA was performed using the TaqMan method. MCs incubated in medium without uPA served as a control. Results are presented as mean ± s.e.m. of three independent experiments.

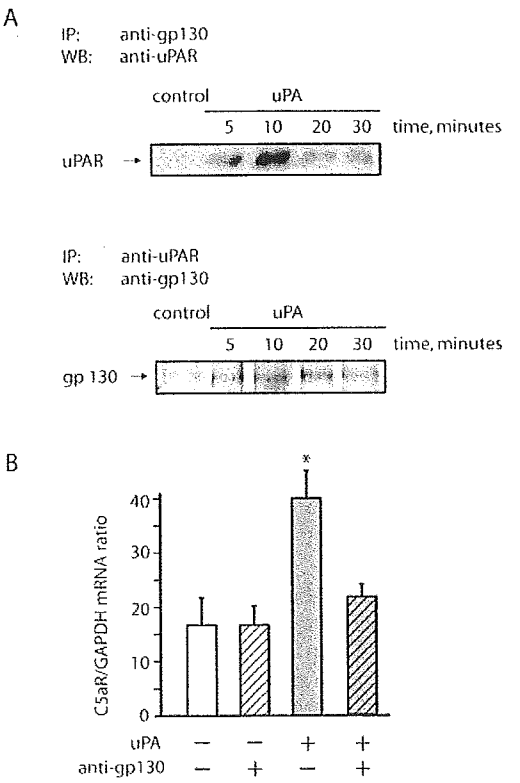

Fig. 8. uPAR utilizes gp130 adaptor protein to mediate C5aR expression in MCs. (A) Quiescent MCs were stimulated with 10 nM uPA for the indicated times or left unstimulated (control), and anti-gp130 (upper panel) or anti-uPAR (lower panel) antibody was used to coimmunoprecipitate gp130 and uPAR from the cell lysates. The immunoprecipitates were then analyzed with anti-uPAR (upper panel) or anti-gp130 antibody (lower panel). (B) RT-PCR analysis of C5aR mRNA was performed using the TaqMan method. RNA was isolated from quiescent MCs incubated for 6 hours with 20 nM uPA or in medium without uPA (control) in the presence or absence of 5 μg/ml of anti-gp130 antibody. Results are presented as mean ± s.e.m. of two independent experiments performed in duplicates for each condition.

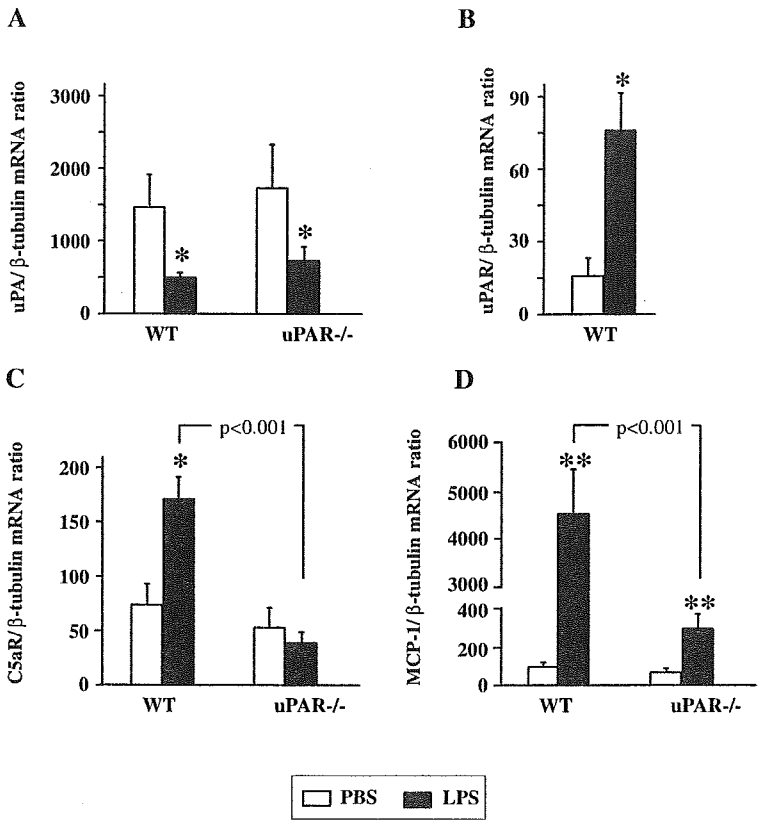

Fig. 9. uPAR is required for C5aR expression in mesangium upon LPS-induced renal inflammation in mice. LPS-induced nephritis was induced in wild-type and *uPAR*$^{-/-}$ mice by an intraperitoneal injection of 50 μg LPS in 200 μl PBS. Animals injected with PBS only, served as a control. 8 hours after challenge the mice were killed, RNA was isolated from kidney glomeruli and used for expression analysis by the TaqMan method. The mRNA levels were analyzed for uPA (A), uPAR (B), C5aR (C) and MCP-1 (D). β-tubulin served as a house-keeping gene. Results are expressed as mean ± s.e.m. (n=6 mice for each group). Significance between PBS controls and LPS-treated animals was determined by Student's t-test (*P<0.05; **P<0.01).

(Koshelnick et al., 1997). Numerous reports provide evidence that activation of Stat3 in response to various stimuli in several cell types is mediated by gp130. These observations point to the probable involvement of gp130 in the uPA-directed Stat3 activation and C5aR upregulation in MCs. To address this hypothesis, we performed immunoprecipitation using anti-gp130 antibody from MCs stimulated with uPA at different time points and determined uPAR in the immunoprecipitates using immunoblotting. Indeed, we observed a specific band for uPAR in the immunoprecipitates (Fig. 8A, upper panel). Specificity of this association was further confirmed in immunoprecipitation experiments using a reverse combination of antibodies, namely anti-uPAR antibody for precipitation and anti-gp130 antibody for western blotting (Fig. 8A, lower panel). The uPAR-gp130 association was uPA-dependent and displayed kinetics very similar to those observed by us for Stat3 and Tyk2 activation. These results suggest that in the uPA-stimulated MCs, uPAR may directly bind to the gp130 adaptor protein, which, in turn, provides a link to the Jak/Stat pathway.

To confirm that gp130 is required to propagate C5aR expression in MCs in response to uPA, cells were pretreated with anti-gp130 blocking antibody and the uPA-directed expression of C5aR was monitored by TaqMan RT-PCR. As expected, no increase in C5aR expression in response to uPA was observed after gp130 blockage (Fig. 8B).

uPAR is required for C5aR expression in mesangium upon LPS-induced renal inflammation in mice

To find out whether our findings might reflect a physiologically relevant process, in vivo studies were performed using a LPS-induced inflammation model. Kidney inflammation was induced by an intraperitoneal injection of LPS into wild-type and uPAR-deficient mice. For control experiments, phosphate-buffered saline (PBS) vehicle was injected. At 8 hours after injections kidney cortex, enriched in glomeruli, was isolated and used for expression analysis. uPA expression was decreased in both wild-type and *uPAR*$^{-/-}$ LPS-treated animals, although there was no difference between these two groups (Fig. 9A). In contrast, uPAR expression in glomeruli of wild-type mice after LPS-induced nephritis was strongly upregulated as compared to control PBS-treated animals (Fig. 9B). Interestingly, while C5aR and MCP-1 were upregulated in inflammed glomeruli of wild-type mice, these responses were abrogated in uPAR-deficient mice (Fig. 9C,D).

Finally, to exclude the possibility that the observed activation of C5aR in glomeruli of LPS-injected mice might be caused by infiltrating neutrophils and macrophages and not restricted to mesangial cells, immunohistochemical studies were performed. This examination revealed the upregulated expression of C5aR localized within mesangium of inflamed glomeruli of wild-type mice (Fig. 10A, upper panels). No infiltrating cells expressing C5aR were identified. The prominent immunohistochemical signal observed in the mesangium of LPS-treated animals was completely abolished in *uPAR*$^{-/-}$ mice with LPS-induced nephritis (Fig. 10A, lower panels). The difference in C5aR expression was further confirmed by a semi-quantification analysis of mesangial immunoreactivity (Fig. 10B).

Discussion

An important challenge in renal cell biology is to understand regulatory signaling pathways that control MC functional changes. Activated MCs play a direct role in the initiation and propagation of inflammatory events within the glomerulus. Recent studies have documented the expression of the complement anaphylatoxin receptors in the kidney (Fayyazi et al., 2000; Abe et al., 2001; de Vries et al., 2003), particularly on MCs (Braun and Davis III, 1998; Wilmer et al., 1998). These findings give a new insight into the mechanisms by which MCs may contribute to the pathogenesis of

glomerulonephritis and other glomeruli-associated kidney disorders. Thus, it is considered that the presence of complement receptors on MCs may mediate their specific interactions with activated complement products, which are decisive factors in tissue damage. However, there is still much that is not known about this process. One of the crucial, but still unexplored aspects, is the mechanism of regulated expression of the complement C5a anaphylatoxin receptor in MCs. This is of special importance, since uncontrolled or improperly activated C5aR expression may be crucial for the pathogenesis of complement-mediated tissue damage. In this study we provide convincing evidence that, in MCs, uPA, via its specific receptor uPAR and the association of uPAR with gp130 adaptor protein, regulates expression of C5aR and modulates C5a-dependent functional responses. The Janus kinase Tyk2 and transcription factor Stat3 serve as downstream components in the signaling cascade resulting in C5aR expression. Our data underscore a new role for uPA/uPAR-related signaling in the initiation and propagation of glomeruli-associated inflammation.

We suggest that at least two interrelated mechanisms are involved: activated expression on MCs of the complement anaphylatoxin C5a receptor and modulation of C5a-directed proinflammatory cytokines release and of cell proliferation. Thus, we show that uPA induces expression of C5aR on human MCs in a dose-dependent and transient fashion at both mRNA and protein levels. This process required functionally active uPAR, as proved by cell pretreatment with uPAR-blocking antibody. We provide evidence that uPA functions as a modulator of the C5aR-dependent processes in human MCs. Thus, we observed a synergistic, uPAR-mediated effect of uPA and C5a on MC proliferation and MCP-1 release, the events that could contribute to the progression of inflammatory renal injury.

We have extended these in vitro observations to an in vivo model of renal inflammation. We show that *uPAR*$^{-/-}$ mice are protected from LPS-induced glomerular inflammation. At the time point examined, no increase in C5aR expression in the mesangium of *uPAR*$^{-/-}$ mice was observed after LPS treatment, in contrast to the findings in wild-type animals. Consistent with these data, expression of MCP-1 was dramatically increased in wild-type animals, whereas only moderate increase was observed in uPAR-deficient mice. Our immunohistological studies demonstrate that under our experimental conditions, namely the low LPS concentration and short time of treatment, rapid upregulation of C5aR was restricted to mesangial cells and preceded LPS-induced leukocyte infiltration into glomeruli.

We investigated the molecular mechanism underlying the revealed uPA/uPAR-related upregulation of C5aR on MCs and delineated the gp130/Tyk2/Stat3 signaling pathway responsible for this effect. Although uPAR has been well documented as an important modulator and orchestrator of signaling events, the functional purpose of uPAR-directed signaling in the cell has only been elucidated in a few studies. One of the obvious limitations in this research field is the cellular specificity of uPA/uPAR-related signaling cascades. Thus, several studies have documented that uPAR-dependent tumor growth involves ERK/MAPK signaling (Liu et al., 2002), whereas FAK signaling mediated tumor dormancy (Ghiso, 2002). In human vascular smooth muscle cells the Tyk2/Stat1 pathway was shown to regulate cell migration and proliferation via a cross-talk with different downstream

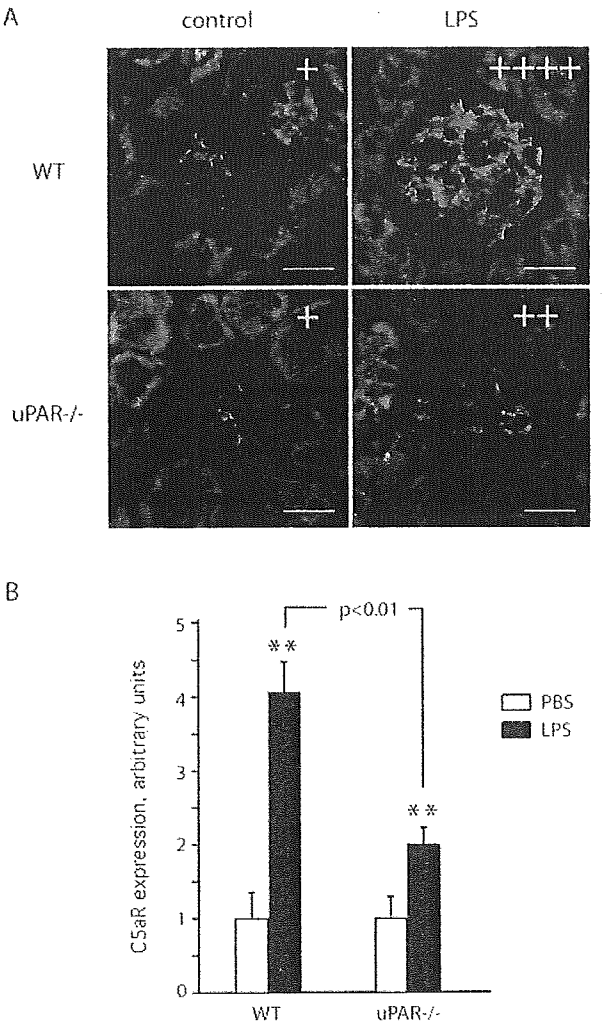

Fig. 10. uPAR is required for C5aR expression in mesangium upon LPS-induced renal inflammation in mice. (A) LPS-induced nephritis was induced in wild-type and *uPAR*$^{-/-}$ mice as described in Fig. 9. 8 hours after challenge the mice were killed and 6 μm cryosections of kidney cortex were stained for C5aR protein expression using anti-C5aR primary antibody and Cy3-conjugated secondary antibodies. Representative microphotographs are shown (6 mice for each group). Bar, 50 μm. (B) Statistical analysis of C5aR expression in mesangium of wild-type and *uPAR*$^{-/-}$ mice with LPS-induced nephritis was performed by evaluating the total number of positively stained glomeruli and the staining intensity (in arbitrary units) as described in the Materials and Methods. Results are expressed as mean ± s.e.m. (n=6 mice for each group). Significance between PBS controls and LPS-treated animals was determined by Student's t-test (*P<0.05; **P<0.01). +, arbitrary units (based on staining intensity using criteria described in Materials and Methods).

signaling cascades (Kusch et al., 2000; Kiian et al., 2003; Kunigal et al., 2003). By contrast, uPA-stimulated migration of rat smooth muscle cells requires activation of MEK and Erk kinases (Degryse et al., 2001). These and other data on the cell specificity of uPAR signaling emphasize the potential for different cell types to respond differently to a given signal. In

light of the multitude of biological functions played by the uPA/uPAR system it is of fundamental importance to determine different cascades of the uPAR-signaling machinery and then to assign particular pathways to particular cells and functions.

Signal transducers and activators of transcription of the Stat family play important roles in regulating immediate-early biological effects initiated by a variety of extracellular ligands including cytokines, chemokines and growth factors (Darnell et al., 1994; Schindler, 1999). Activation of latent, cytoplasmic, or membrane-associated Stat proteins requires their tyrosine phosphorylation, which in most cases depends on the activity of protein tyrosine kinases of the Janus family (Ziemiecki et al., 1994). After their phosphorylation, Stat proteins form homo- or heterodimers in order to translocate to the nucleus, where site-specific binding to enhancer elements leads to gene activation. uPA/uPAR has been documented to utilize Jak/Stat signaling in several cell types. Thus, in human kidney epithelial tumor cells uPAR is associated with the Jak1/Stat1 pathway, although cellular effects of this signaling remained unexplored (Koshelnick et al., 1997). In human vascular smooth muscle cells, the Tyk2/Stat1 pathway modulates, as mentioned above, uPA/uPAR-directed cell migration and proliferation.

In this study, we demonstrate that Stat3 is a key signaling molecule, which mediates upregulated expression of C5aR in human MCs in response to uPA. Our results show that uPA induces tyrosine phosphorylation of Stat3, but not other Stats, and its nuclear translocation. Obviously, these processes are required to induce uPA-related C5aR expression, since MCs expressing the Stat3 inactive mutant were unable to express C5aR when stimulated with uPA. Our studies on Janus kinases indicate that Tyk2 is responsible for the observed Stat3 tyrosine phosphorylation. Indeed, we observed fast and reversible Tyk2 activation in MCs in response to uPA, whereas Jak1, Jak2 and Jak3 were not affected. The kinetics of this activation correlates with those of the uPA-induced Stat3 phosphorylation, assuming that both processes are coordinated in time. Furthermore, MCs expressing kinase-dead Tyk2 mutants did not respond to uPA with Stat3 activation and C5aR expression, indicating a decisive role for Tyk2 kinase activity in these processes. Both Tyk2 and Stat3 activation by uPA required native cell surface uPAR, since no Tyk2/Stat3 phosphorylation was observed in uPARsi-MC where uPAR expression was downregulated. Our results confirm and extend the findings of others that expression of some G protein-coupled receptors is regulated by the Jak/Stat3 pathway (Senga et al., 2003).

Stat3 protein plays a central role in transmitting a multitude of different processes initiated by the IL-6 cytokine family (French et al., 2002). Moreover, IL-6 has been shown to mediate expression of C5aR in several cell types (Riedemann et al., 2003). Therefore, it was tempting to speculate that induction of the Tyk2/Stat3 pathway followed by the upregulation of C5aR might result from the uPA-triggered IL-6 activation, instead of reflecting a direct effect of uPA. To verify this hypothesis, separate experiments have been performed. Thus, we measured, using specific ELISA, IL-6 secretion from MCs stimulated dose-dependently with uPA for different times and examined expression of both α- and β-subunits of the IL-6 receptor in uPA-stimulated cells. No changes were observed (data not shown) thus indicating that C5aR expression in MCs is indeed attributed to the uPA/uPAR-induced signaling.

Although the revealed mechanism of uPA-mediated C5aR expression is IL-6 independent, uPAR utilizes gp130 protein, a signal transducing subunit of the receptor complexes of the IL-6 cytokine family, as a membrane interactor to mediate C5aR expression. In order to identify a transmembrane protein, which might serve as an adaptor for uPAR in mesangial cells and therefore couple uPAR to the pathway required for C5aR expression, several experiments have been performed aiming at analyzing uPAR-interacting proteins. Thus, we used the a325 peptide that dissociates uPAR-integrin complexes, FPR-family receptor inhibiting peptides, and pharmacological inhibitors of tyrosine kinase receptors. No effect on the uPA-mediated C5aR expression was observed in all these experiments (data not shown). Instead, we found that uPAR is associated in an uPA-dependent fashion with gp130. We also provide evidence that this association is required to mediate C5aR expression in MCs in response to uPA.

A relevant question regarding the functional role of uPAR signaling in C5aR regulation in MCs is the source of uPA in glomeruli. In our in vivo experiments we observed a decrease in uPA expression in mesangium of both wild-type and uPAR-deficient mice treated with LPS. These results correlate with the data of others on the reduction in urinary and renal uPA in LPS-injected mice, suggesting that an imbalanced fibrinolytic system might participate in kidney dysfunction upon inflammation (Yamamoto and Loskutoff, 1996). By contrast, we noticed strong upregulation of uPAR expression in inflammed mesangium of wild-type animals. Thus, it appears that the regulation of the C5aR expression pathway may result from the uPAR-mediated uptake of uPA via the increased number of uPAR available for its ligand on the surface of MCs. A paracrine loop of stimulation cannot be excluded, although the source of uPA in mesangium during inflammation remains to be elucidated.

In summary, the results of the present study demonstrate that uPA, via the uPAR-directed signaling machinery, regulates expression of the anaphylatoxin C5a receptor on MCs, and modulates C5a-dependent functional responses. These findings suggest the possibility that MCs may be therapeutic targets for inhibiting complement-mediated glomerular damage.

We thank Peter Carmeliet and Mieke Dewerchin (Leuven, Belgium) for providing uPA- and uPAR-deficient mice, Didier Trono (Geneva, Switzeland) for the lentivirus production plasmids, Ying Wei (San Francisco, CA, USA) for providing a325 and random peptides and Francesco Blasi for FPR-inhibiting peptide. This work was supported by grant Sh 98/1-1 from the Deutsche Forschungsgemeinschaft.

References

Abe, K., Miyazaki, M., Koji, T., Furusu, A., Nakamura-Kurashige, T., Nishino, T., Ozono, Y., Harada, T., Sakai, H. and Kohno, S. (2001). Enhanced expression of complement C5a receptor mRNA in human diseased kidney assessed by in situ hybridization. *Kidney Int.* **60**, 137-146.

Abraham, E., Gyetko, M. R., Kuhn, K., Arcaroli, J., Strassheim, D., Park, J. S., Shetty, S. and Idell, S. (2003). Urokinase-type plasminogen activator potentiates lipopolysaccharide-induced neutrophil activation. *J. Immunol.* **170**, 5644-5651.

Aramugam, T. V., Shiels, I. A., Strachan, A. I., Abbenante, G., Fairlie, D. P. and Taylor, S. M. (2003). A small molecule C5a receptor antagonist protects kidneys for ischemia/reperfusion injury in rats. *Kidney Int.* **63**, 134-142.

Blasi, F. and Carmeliet, P. (2002). uPAR: a versatile signalling orchestrator. *Nat. Rev. Mol. Cell Biol.* **3**, 932-943.
Braun, M. and Davis, A. E., III (1998). Cultured human mesangial cells express the C5a receptor. *Kidney Int.* **54**, 1542-1549.
Chatterjee-Kishore, M., Van den Akker, F. and Stark, G. R. (2000). Association of STATs with relatives and friends. *Trends Cell Biol.* **10**, 106-110.
Darnell, J. E. J., Kerr, I. M. and Stark, G. R. (1994). Jak-STAT pathways and transcriptional activation in response to IFNs and other extracellular signaling proteins. *Science* **264**, 1415-1421.
de Vries, B., Koehl, J., Leclercq, K. G., Wolfs, T. G. A. M., van Bijnen, A. A. J. H. M., Heeringa, P. and Buurman, W. (2003). Complement factor C5a mediates renal ischemia-reperfusion injury independent from neutrophils. *J. Immunol.* **170**, 3883-3889.
Degryse, B., Orlando, S., Resnati, M., Rabbani, S. A. and Blasi, F. (2001). Urokinase/urokinase receptor and vitronectin/alphav betta 3 integrin induced chemotaxis and cytoskeleton reorganization through different signaling pathways. *Oncogene* **20**, 2032-2043.
Dumler, I., Weis, A., Mayboroda, O. A., Maasch, C., Jerke, U., Haller, H. and Gulba, D. C. (1998). The Jak/Stat pathway and urokinase receptor signaling in human aortic vascular smooth muscle cells. *J. Biol. Chem.* **273**, 315-321.
Fayyazi, A., Scheel, O., Schweyer, S., Oppermann, M., Goetze, O., Radzun, H. J. and Zwirner, J. (2000). The C5a receptor is expressed in normal renal proximal tubular but not in normal pulmonary or hepatic epithelial cells. *Immunology* **99**, 38-45.
French, J. D., Tschumper, R. C. and Jelinek, D. F. (2002). Analysis of IL-6-mediated growth control of myeloma cells using a gp130 chimeric receptor approach. *Leukemia* **16**, 1189-1196.
Gerard, C. and Gerard, N. P. (1994). C5a anaphylatoxin and its seven transmembrane-segmented receptor. *Ann. Rev. Immunol.* **12**, 775-808.
Ghiso, A. J. A. (2002). Inhibition of FAK signaling activated by urokinase receptor induces dormancy in human carcinoma cells in vivo. *Oncogene* **21**, 2513-2524.
Gyetko, M. R., Chen, G. H., McDonald, R. A., Goodman, R., Huffnagle, G. B., Wilkinson, C. C., Fuller, J. A. and Toews, G. B. (1996). Urokinase is required for the pulmonary inflammatory response to Cryptococcus neoformans. A murine transgenic model. *J. Clin. Invest.* **97**, 1818-1826.
Gyetko, M. R., Sud, S., Kendall, T., Fuller, J. A., Newstead, M. W. and Standiford, T. J. (2000). Urokinase receptor-deficient mice have impaired neutrophil recruitment in response to pulmonary Pseudomonas aeruginosa infection. *J. Immunol.* **165**, 1513-1519.
Gyetko, M. R., Sud, S., Chen, G. H., Fuller, J. A., Chensue, S. W. and Toews, G. B. (2002). Urokinase-type plasminogen activator is required for the generation of a type 1 immune response to pulmonary Cryptococcus neoformans infection. *J. Immunol.* **168**, 801-809.
Kiian, I., Tkachuk, N., Haller, H. and Dumler, I. (2003). Urokinase-induced migration of human vascular smooth muscle cells requires coupling of the small GTPases RhoA and Rac1 to the Tyk2/PI3-K signalling pathway. *Thromb. Haemost.* **89**, 904-914.
Koshelnick, Y., Ehart, M., Hufnagl, P., Heinrich, P. C. and Binder, B. R. (1997). Urokinase receptor is associated with the components of the JAK1/STAT1 signaling pathway and leads to activation of this pathway upon receptor clustering in the human kidney epithelial tumor cell line TCL-598. *J. Biol. Chem.* **272**, 28563-28567.
Kunigal, S., Kusch, A., Tkachuk, N., Tkachuk, S., Jerke, U., Haller, H. and Dumler, I. (2003). Monocyte-expressed urokinase inhibits vascular smooth muscle cell growth by activating Stat1. *Blood* **102**, 4377-4383.
Kusch, A., Tkachuk, S., Haller, H., Dietz, R., Gulba, D. C., Lipp, M. and Dumler, I. (2000). Urokinase-dependent activation of phosphatidylinositol 3-kinase: intercation with Tyk2 and requirement for human vascular smooth muscle cell migration. *J. Biol. Chem.* **275**, 39466-39473.
Liu, D., Ghiso, J. A. A., Estrada, Y. and Ossowski, L. (2002). EGFR is a transducer of the urokinase receptor initiated signal that is required for in vivo growth of a human carcinoma. *Cancer Cell* **1**, 445-457.
May, A. E., Kanse, S. M., Lund, L. R., Gisler, R. H., Imho, F. B. A. and Preissner, K. T. (1998). Urokinase receptor (CD87) regulates leukocyte recruitment via β2 integrins in vivo. *J. Exp. Med.* **188**, 1029-1037.
Mondino, A. and Blasi, F. (2004). uPA and uPAR in fibrinolysis, immunity and pathology. *Trends Immunol.* **25**, 450-455.
Riedemann, N. C., Neff, T. A., Guo, R.-F., Bernacki, K. D., Laudes, I. J., Sarma, J. V., Lambris, J. D. and Ward, P. A. (2003). Protective effects of IL-6 blockade in sepsis are linked to reduced C5a receptor expression. *J. Immunol.* **170**, 503-507.
Schindler, C. (1999). Cytokines and JAK-STAT Signaling. *Exp. Cell Res.* **253**, 7-14.
Senga, T., Iwamoto, S., Yoshida, T., Adachi, K., Azuma, E., Hamaguchi, M. and Iwamoto, T. (2003). LISSIG is a novel murine leukocyte-specific GPCR that is induced by the activation of STAT3. *Blood* **101**, 1185-1187.
Sitrin, R. G., Shollenberger, S. B., Strieter, R. M. and Gyetko, M. R. (1996). Endogenously produced urokinase amplifies tumor necrosis factor-alpha secretion by THP-1 mononuclear phagocytes. *J. Leukoc. Biol.* **59**, 302-311.
Werfel, T., Zwirner, J., Oppermann, M., Sieber, A., Begemann, G., Drommer, W., Kapp, A. and Gotze, O. (1996). CD88 antibodies specifically bind to C5aR on dermal CD117+ and CD14+ cells and react with a desmosomal antigen in human skin. *J. Immunol.* **157**, 1729-1735.
Wilmer, W. A., Kaumaya, P. T., Ember, J. A. and Cosio, F. G. (1998). Receptors for the anaphylatoxin C5a (CD88) on human mesangial cells. *J. Immunol.* **160**, 5646-5652.
Yahata, Y., Shirakata, Y., Tokumaru, S., Yamasaki, K., Sayama, K., Hanakawa, Y., Detmar, M. and Hashimoto, K. (2003). Nuclear translocation of phosphorylated STAT3 is essential for vascular endothelial growth factor-induced human dermal microvascular endothelial cell migration and tube formation. *J. Biol. Chem.* **278**, 40026-40031.
Yamamoto, K. and Loskutoff, D. J. (1996). Fibrin deposition in tissues from endotoxin-treated mice correlates with decreases in the expresssion of urokinase-type but not tissue-type plasminogen activator. *J. Clin. Invest.* **97**, 2440-2451.
Ziemiecki, A., Harpu, A. G. and Wilks, A. F. (1994). JAK protein tyrosine kinases: their role in cytokine signalling. *Trends Cell Biol.* **4**, 207-212.

Journal of Neuroscience Research 81:163–171 (2005)

Suppression of Stat3 Promotes Neurogenesis in Cultured Neural Stem Cells

Feng Gu,[1] Ryuji Hata,[1]* Yong-Jie Ma,[1] Junya Tanaka,[2] Noriaki Mitsuda,[2] Yoshiaki Kumon,[3] Yasushi Hanakawa,[4] Koji Hashimoto,[4] Koichi Nakajima,[5] and Masahiro Sakanaka[1]

[1]Department of Anatomy, Ehime University School of Medicine, Shitsukawa, Toon, Ehime, Japan
[2]Department of Physiology, Ehime University School of Medicine, Shitsukawa, Toon, Ehime, Japan
[3]Department of Neurosurgery, Ehime University School of Medicine, Shitsukawa, Toon, Ehime, Japan
[4]Department of Dermatology, Ehime University School of Medicine, Shitsukawa, Toon, Ehime, Japan
[5]Department of Immunology, Institute of Geriatrics and Medical Science, Osaka City University Medical School, Osaka, Japan

To investigate the effects of signal transducer and activator of transcription 3 (Stat3) on neural stem cell fate, stem cells were inoculated with an adenovirus vector expressing dominant negative form of Stat3 (Stat3F). One day later, a promoter assay revealed significant reduction of the transcriptional level in the transfected cells. Three days later, Western blot analysis and immunocytochemical analysis revealed that the protein level of microtubule-associated protein (MAP)2 and the number of MAP2-positive cells were increased significantly in the transfected cells whereas the protein level of glial fibrillary acidic protein (GFAP) and the number of GFAP-positive cells were decreased significantly. In addition, mRNA levels of Notch family members (Notch1, 2, and 3) and of inhibitory basic helix-loop-helix (bHLH) factors (Hes5, Id2, and Id3) were significantly downregulated at 3 days after viral inoculation with Stat3F; however, mRNA levels of bHLH determination factors (Math1 and Neurogenin3) and bHLH differentiation factors (NeuroD1 and NeuroD2) were significantly upregulated. These data indicated that suppression of Stat3 directly induced neurogenesis and inhibited astrogliogenesis in neural stem cells.

Key words: Stat3; neural stem cell; neurogenesis; astrogliogenesis

Investigations of signal transduction from interferon (IFN) receptors led to the discovery of the first member of the signal transducer and activator of transcription (Stat) protein family, Stat1 (Darnell et al., 1994). Stat proteins exist as cytoplasmic unphosphorylated monomers of cells. In response to specific stimuli, they can be phosphorylated, and can homo- or heterodimerize. Dimerized Stat proteins then can translocate to the nucleus, where they bind to specific consensus sequences to control various target genes (Levy and Lee, 2002). Stat3 was first described as acute-phase response factor (APRF) from interleukin (IL)-6–stimulated hepatocytes (Wegenka et al., 1993). APRF is a DNA-binding protein that can interact selectively with an enhancer element in the promoter of acute-phase genes, known as the acute-phase response element (APRE).

The function of Stat3 has been investigated extensively and IL-6–type cytokines such as IL-6, leukemia inhibitory factor (LIF), and ciliary neurotrophic factor (CNTF) evoke several distinct responses in different cells. Stat3 is critical for inducing acute-phase responses in hepatoma cells as well as for activating terminal differentiation and inducing growth arrest in monocytes (Heinrich et al., 1998). Stat3 is also essential for epithelial cell apoptosis and involution in the postlactating mammary gland (Horvath, 2000). Recently, increasing evidence indicates that Stat3 can maintain the propagation and pluripotency of embryonic stem cells (Matsuda et al., 1999; Burdon et al., 2002). Targeted disruption of the Stat3 gene in mice results in early embryonic lethality (Takeda et al., 1997). In addition, ectopic overexpression of the dominant negative form of Stat3 in embryonic stem cells leads to a loss of pluripotency and enhanced cell differentiation (Niwa et al., 1998).

Neural stem cells are thought to undergo differentiation into neurons and astrocytes under the influence of Stat3; however, the effect of Stat3 on neural stem cell fate remains controversial. On the one hand, Stat3 can

Contract grant sponsor: Ministry of Education, Science and Culture; Contract grant sponsor: Daiwa Securities Health Foundation; Contract grant sponsor: Mitsui Sumitomo Insurance Welfare Foundation.

*Correspondence to: Ryuji Hata, Department of Anatomy and Neuroscience, Ehime University School of Medicine, Shitsukawa, Toon, Ehime 791-0295, Japan. E-mail: hata@m.ehime-u.ac.jp

Received 22 November 2004; Revised 3 April 2005; Accepted 12 April 2005

Published online 9 June 2005 in Wiley InterScience (www.interscience.wiley.com). DOI: 10.1002/jnr.20561

promote glial differentiation in neural stem cells in response to CNTF and LIF (Bonni et al., 1997; Rajan and McKay, 1998). On the other hand, LIF generates neurons rather than astrocytes from early cortical precursors despite the presence of downstream signaling molecules (Molne et al., 2000), and Stat3 is required for the neurotrophic effects of CNTF and LIF on developing sensory neurons (Alonzi et al., 2001).

To confirm the direct effect of Stat3 on the neural stem cell, adenovirus vector expressing dominant negative form of Stat3 (Stat3F) was applied. In this mutant (Stat3F), the tyrosine residue at amino acid position 705 of murine Stat3 is mutated to phenylalanine. Stat3F binds to the gp130 receptor, which in turn leads to competitively inhibited phosphorylation of endogenous Stat3 upon activation of the gp130 receptor. When expressed at high levels, Stat3F has been shown to block the activation of endogenous Stat3 in various cell types (Nakajima et al., 1996; Bonni et al., 1997; Ozawa et al., 2004). We demonstrate that Stat3F overexpression directly promotes neurogenesis and inhibits astrogliogenesis in neural stem cells.

MATERIALS AND METHODS

All experiments proceeded according to the Guidelines for Animal Experimentation at Ehime University School of Medicine and were approved by our institutional Ethics Committee.

Adenoviral Vectors

To make Stat3F, the tyrosine residue at 705 of Stat3 was replaced with phenylalanine (Y705F; Nakajima et al., 1996). A recombinant adenovirus expressing dominant negative form of murine Stat3 (Stat3F) was constructed as described previously (Masumura et al., 2000). In brief, Stat3F DNA (Nakajima et al., 1996) was excised and the resultant expression units were inserted at the *Swa*I site of the cosmid vector, pAxCAwt (RBD: 1678, Bio Resource Center, Riken, Tokyo, Japan). Cosmid DNA was cotransfected with the DNA-terminal protein complex into human kidney 293 cells to generate a recombinant virus (Ad.Stat3F). An adenovirus expressing β-galactosidase (Ad.LacZ) was provided by Dr. Izumu Saito (University of Tokyo, Tokyo, Japan). Each recombinant virus was propagated in 293 cells and purified by CsCl step-gradient ultracentrifugation. Viral titers were determined using the modified end-point cytopathic effect assay (Kanegae et al., 1994).

Neurosphere Generation and Maintenance

Neural stem cells were isolated from rat embryo (day 17–18). The embryonic rat brain was cleared of meninges, and striatal tissue from both hemispheres was dissected using fine forceps. The tissue was mechanically triturated and cell suspensions were seeded in 9-cm dishes (Sumilon MS13900; Sumitoko Bakelite Co. Ltd., Tokyo, Japan) in growth medium composed of Dulbecco's modified Eagle medium (DMEM; Sigma Chemical Co., St. Louis, MO) containing 0.2 mg/ml bovine serum albumin (BSA, A-7638; Sigma, St. Louis, MO), 10 mM HEPES, 4.5 mg/ml glucose, 5 μg/ml insulin, 5 nM sodium selenite, 5 μg/ml transferrin, and 40 ng/ml of human recombinant epidermal growth factor (EGF; Upstate Biotechnology, Lake Placid, NY). Antibiotics and antimycotics (penicillin 100 units/ml, streptomycin 100 μg/ml, and amphotericin B 0.25 μg/ml) were also included. Neural stem cells were grown as neurospheres.

Viral Inoculation and Differentiation of Neuronal Progenitor Cells

Five days after seeding, neurospheres were dissociated mechanically and neural stem cells were exposed to adenovirus vector expressing Stat3F or LacZ (multiplicity of infection = 10) for 1 hr in the same growth medium. Some were transfected additionally with the Stat3 reporter plasmids for luciferase promoter assay. Cells were then seeded at a density of 2×10^6/well on poly-L-lysine coated 12-well dishes in differentiating medium (Neurobasal medium; Invitrogen, Gaithersburg, MD) containing B27 supplement (Invitrogen), all-*trans*-retinoic acid (10^{-7} M), 2 mM L-glutamine, and antibiotics (penicillin 50 units/ml and streptomycin 50 μg/ml).

For the positive control, neural stem cells were transfected with the Stat3 reporter plasmids for luciferase promoter assay without exposure to adenovirus vector and incubated in the differentiating medium in the presence of LIF (30 ng/ml) and basic fibroblast growth factor (bFGF; 10 ng/ml). Treatment with LIF and bFGF has been reported to activate Stat3 and promote astrogliosis in the neural stem cells (Molne et al., 2000).

Luciferase Promoter Assay

The constructs of the Stat3 reporter plasmids have been described elsewhere (Nakajima et al., 1993, 1996). In brief, the Stat3 reporter plasmid contains four copies of APRE in front of the minimal junB promoter linked to the luciferase gene. The response element was the APRE of the rat α2-macroglobulin gene, 5′-GCGCCTTCTGGGAAGATCCT-TACGGGAATTCAG-3′. Viral inoculated neurospheres were washed once in cold phosphate-buffered saline (PBS), and resuspended in the specified electroporation buffer to a final concentration of 1×10^7 cells/ml. Stat3 reporter plasmid (10 μg) and 4 μg of pRL-TK (Promega, Madison, WI) internal control plasmid DNA were mixed with 0.1 ml of cell suspension, transferred to a 2.0-mm electroporation cuvette, and electroporated with an Amaxa Nucleofector apparatus (Amaxa, Cologne, Germany). One day after electroporation, the activities of firefly luciferase from Stat3 promoter-luciferase plasmid and renilla luciferase from pRL-TK plasmid in the cell extracts were evaluated by Dual-luciferase assay kit (Promega) with a luminometer (TD-20/20; Turner Designs, USA). The relative firefly luciferase activities were calculated by normalizing transfection efficiency according to the renilla luciferase activities.

Immunoblot Analysis

Immunoblot proceeded according to Laemmli (1970). Cells were solubilized in Laemmli's lysis buffer containing 2% SDS. The suspension was resolved by electrophoresis, trans-

TABLE I. Sequences, Annealing Temperatures, Cycle Numbers, and PCR Product Sizes for Each Pair of Probes*

Primer	Sequence (5′ → 3′)	Anneal Tm (°C)	Cycle	Product size (bp)
β-actin	F: aga aga gct atg agc tgc ctg acg	55	20	312
	R: tac ttg cgc tca gga gga gca atg			
Notch1	F: tgt gac agc cag tgc aac tc	57	32	547
	R: tgg cgc tct gga agc att gc			
Notch2	F: gcc gtc aga ctg gag act tc	57	32	640
	R: gcg tag ccc ttc aga cac tc			
Notch3	F: agt cac tgc gaa cag gag gt	57	32	514
	R: agg gga aca gag cag tct ga			
Hes1	F: cga gcg tgt tgg gga agt a	57	35	101
	R: agt gcg cac ctc ggt gtt a			
Hes5	F: gat gct cag tcc caa gga ga	57	35	336
	R: cgc tgg aag tgg taa agc ag			
Id1	F: gat cat gaa ggt cgc cag tag	57	32	218
	R: gct cct tga ggc gtg agt ag			
Id2	F: ctc caa gct caa gga act gg	57	32	207
	R: atg ctg atg tcc gtg ttc ag			
Id3	F: ctg tcg gaa cgt agc cta gc	57	32	177
	R: gtc tat gac acg ctg cag ga			
Mash1	F: aag tca gcg gcc aag cag gtc aag	57	32	245
	R: cgc agc gtc tcc acc ttg ctc atc t			
Math1	F: ttc cag caa aca ggt gaa tg	57	35	132
	R: tgg aca gct tct tgt cgt tg			
Neurogenin3	F: tgc ctc cag acg caa ttt ac	57	38	209
	R: ctc cac gcg gga cta gag ta			
NeuroD	F: cca gac ctc gtc tcc ttt gta	57	35	314
	R: ggg ctg gtg caa tca gtt ag			
NeuroD2	F: ggc cga aga aac gca aga tg	57	33	265
	R: gca cag agt ctg cac gta gg			

*Anneal Tm, annealing temperature; F, forward; R, reverse

ferred to nitrocellulose sheets, and immunoblotted using a rabbit polyclonal antibody against glial fibrillary acidic protein (GFAP, G9269; Sigma) or mouse monoclonal antibodies against β-actin (A5441; Sigma), Stat3 (sc-8019; Santa Cruz), pStat3 (Tyr705 phosphorylated Stat3, sc-8059; Santa Cruz), microtubule-associated protein 2 (MAP2, SMI 52; Sternberger Monoclonals Inc., Lutherville, MD), Tuj1 (MMS-435P; Covance Research, Berkeley, CA), and Nestin (MAB353; Chemicon, Temecula, CA) proteins.

The second antibodies were alkaline-phosphatase conjugated anti-rabbit IgG for the rabbit polyclonal antibody or alkaline-phosphatase conjugated anti-mouse IgG for the mouse monoclonal antibodies. The density of immunoreactive bands was measured using NIH Image software (National Institutes of Health, Bethesda, MD) as described previously (Gu et al., 2003).

Immunocytochemistry

Cells were washed with PBS and fixed for 30 min with 4% paraformaldehyde in 0.1 M phosphate buffer (pH 7.4). After three washes with PBS, the samples were incubated with 10% normal goat serum dissolved in PBS. Either a primary mouse monoclonal antibody against MAP2 (Sternberger Monoclonals) or a rabbit polyclonal antibody against GFAP (Sigma) was incubated with the samples at 4°C overnight. The samples were washed three times with PBS, incubated with rhodamine-conjugated goat anti-mouse IgG (ICN, Irvine, CA) or fluorescein-5-isothiocyanate (FITC)-conjugated goat anti-rabbit IgG (ICN) for 30 min at room temperature, washed three times with PBS, and mounted in Vectashield (Vector Labs, Burlingame, CA). The cells were counterstained with Hoechst 33342 (B2261; Sigma) to identify nuclei.

RT-PCR

Cells were washed with PBS and total RNA was extracted using Isogen (Nippon Gene, Tokyo, Japan). Total RNA was digested with DNase, and then single-stranded cDNA was obtained using oligo dT primers and Moloney murine leukemia virus reverse transcriptase (Life Technologies, Rockville, MD). PCR proceeded using Ex Taq polymerase (Takara, Tokyo, Japan). The synthesized cDNA was amplified under the following conditions: initial denaturation 94°C, 5 min; denaturation 94°C, 1 min; annealing, 55–57°C, 1.5 min; and extension 72°C, 1.5 min for 20–38 cycles. PCR conditions were optimized by varying the annealing temperature and cycle number to determine the linear amplification range. Amplification products were identified by size and confirmed by DNA sequencing. Table I summarizes the primer sequences, annealing temperature, cycle number, and PCR product size for each pair of probes. The PCR products separated on 3% agarose gels were visualized by staining with ethidium bromide and semiquantified using the NIH Image analysis system (National Institutes of Health).

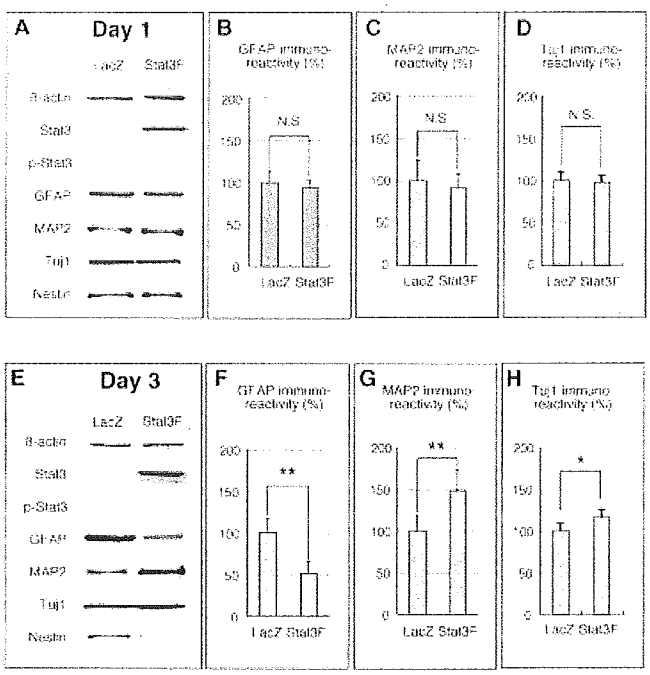

Fig. 1. Effects of the dominant negative form of the signal transducer and activator of transcription 3 (Stat3F) on differentiation of neural stem cells 1 and 3 days after inoculation. Neural stem cells were inoculated with adenovirus vectors expressing Stat3F or β-galactosidase (LacZ). Protein levels were determined by Western blotting 1 or 3 days later. Data were obtained from five independent measurements. Values represent means ± standard deviation. NS, no significant difference; $*P < 0.05$ and $**P < 0.01$, differs significantly vs. LacZ-treated control.

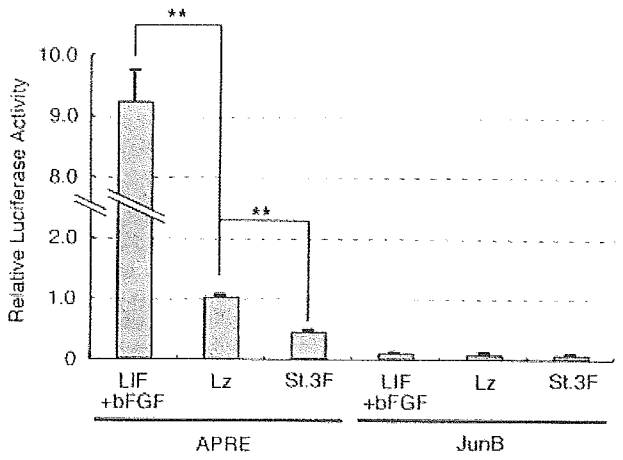

Fig. 2. Specific inhibition of signal transducer and activator of transcription 3 (Stat3) activity by the dominant negative form of Stat3 (Stat3F). Neural stem cells were inoculated with adenovirus vectors expressing Stat3F(Ad.St3F) or β-galactosidase (Ad.LacZ). For the positive control, neural stem cells were treated with leukemia inhibitory factor (LIF; 30 ng/ml) and basic fibroblast growth factor (bFGF, 10 ng/ml; LIF+bFGF). Ad.St3F-treated, Ad.LacZ-treated, or LIF+bFGF-treated neural stem cells were transfected with the Stat3 reporter plasmid (APRE) or Stat3 control plasmid (JunB). APRE: Stat3 reporter plasmid containing four copies of acute phase responsive element in front of the minimal junB promoter linked to the luciferase gene. JunB: Stat3 control plasmid containing the minimal junB promoter linked to the luciferase gene. Data were obtained from five independent measurements. Values were normalized to transfection efficiency and represent means ± standard deviation. Differences in relative luciferase activity were compared using one-way ANOVA followed by Bonferroni's multiple comparison test. $**P < 0.01$, significantly different from Ad.LacZ-treated control.

Statistical Analysis

Data obtained from five independent measurements are presented as means ± standard deviation (SD). If not indicated, differences were evaluated by Mann-Whitney *U*-test for statistical significance. A *P* value below 0.05 was considered statistically significant.

RESULTS

Suppression of Stat3 Cell Signaling Machinery After Viral Inoculation

We initially examined whether neural stem cells expressed Stat3 protein after inoculation with adenovirus vectors. At 1 or 3 days after viral inoculation, cells were homogenized in lysis buffer and immunoblotted with antibody against Stat3, Tyr-705-phosphorylated Stat3 (p-Stat3), and β-actin.

One day after inoculation (Fig. 1A), the Stat3 protein was expressed in the Ad.Stat3F-treated cells, whereas little expression of p-Stat3 was evident. Neither Stat3 nor p-Stat3 protein, however, was expressed in the Ad.LacZ-treated cells. Three days after inoculation (Fig. 1E), the expression level of Stat3 was higher (about 4.2-fold at 1 day after inoculation); however, p-Stat3 was little expressed in the Ad.Stat3F-treated cells. On the contrary, neither Stat3 nor p-Stat3 protein was detected in the Ad.LacZ-treated cells. These data showed that after viral inoculation, the dominant negative form of Stat3 protein was actually overexpressed in neural stem cells although the activated form of Stat3 (p-Stat3) was not.

To confirm whether Ad.Stat3F could inhibit Stat3 function in the neural stem cells, we introduced the minimal junB reporter constructs with or without four copies of APRE into the Ad.Stat3F-treated or Ad.LacZ-treated cells. One day later, a dual luciferase assay was carried out. Luciferase activity in the Ad.Stat3F-treated cells was significantly lower (55.2% reduction) than it was in the Ad.LacZ-treated cells after transfection of the Stat3 reporter plasmid (minimal junB promoter with four copies of APRE; Fig. 2). In addition, luciferase activity in the positive control cells (LIF+bFGF-treated cells) was remarkably higher (about 9.2-fold) than that in the Ad.LacZ-treated cells. Moreover, the low level of relative luciferase activities could be detected after transfection of the control reporter plasmid (minimal junB promoter without APRE) in three groups (0.69% in LIF+bFGF-treated control, 5.5% in Ad.LacZ-treated control, and 3.7% in Ad.Stat3F-treated control; Fig. 2). These results supported the notion that Stat3F could work as a dominant negative regulator in the neural stem cells.

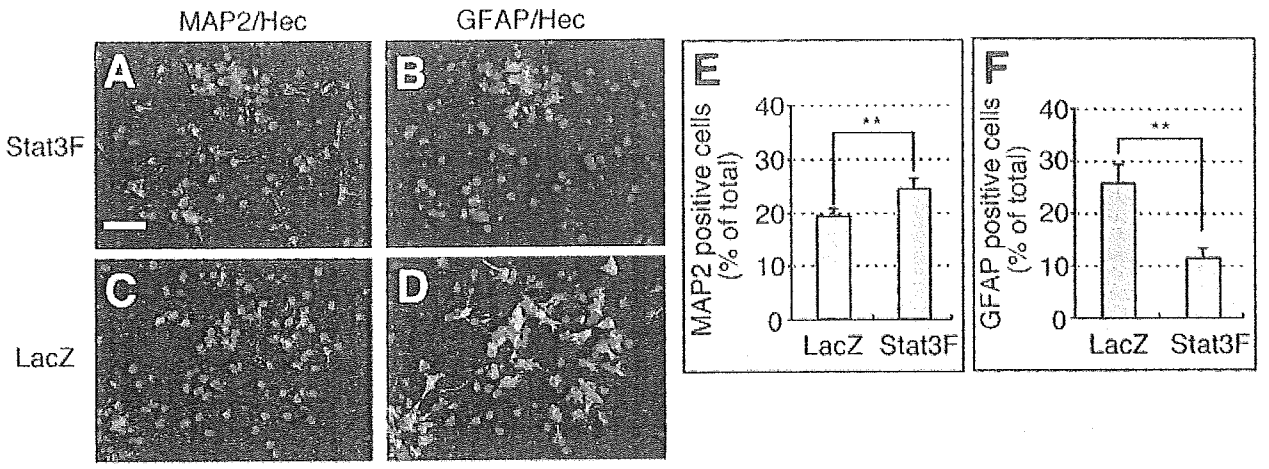

Fig. 3. Effects of dominant negative form of the signal transducer and activator of transcription 3 (Stat3F) on differentiation of neural stem cells 3 days after inoculation. Neural stem cells were inoculated with the adenovirus vector expressing Stat3F or β-galactosidase (LacZ). Three days later, expression of differentiation markers was evaluated by immunostaining with antibody against microtubule-associated protein 2 (MAP2; **A, C**; red) or glial fibrillary acidic protein (GFAP; **B, D**; green). Hec, Hoechst 33342 nuclear staining (blue). Scale bar = 100 μm. Data were obtained from five independent measurements. Values represent means ± standard deviation. $^{**}P < 0.01$, differs significantly vs. LacZ-treated control.

Promotion of Neurogenesis and Inhibition of Astrogliogenesis by Suppression of Stat3

We then evaluated whether suppression of Stat3 cell signaling machinery could modulate the differentiation of neural stem cells. At 1 or 3 days after inoculation, cells were homogenized in lysis buffer and immunoblotted with antibody against MAP2 and Tuj1, which are specific markers for neurons, and GFAP, which is a specific marker of astrocytes. Densitometric analysis revealed that 1 day after inoculation (Fig. 1B–D), the protein levels of GFAP, MAP2, and Tuj1 did not differ between cells treated with either Ad.LacZ or Ad.Stat3F. At 3 days after inoculation, however, the level of GFAP was reduced significantly by 47.5% of the Ad.LacZ-treated control level (Fig. 1F). Furthermore, the levels of MAP2 and Tuj1 proteins in the Ad.Stat3F-treated cells significantly increased up to 148% and 116% of the Ad.LacZ-treated control level, respectively (Fig. 1G,H). We therefore speculated that suppression of Stat3 influenced the differentiation fate of neural stem cells.

To confirm this notion, we immunocytochemically examined whether Stat3F overexpression could affect the number of MAP2-positive neurons or GFAP-positive astrocytes (Fig. 3A–D). Hoechst 33382 staining determined individual nuclei in the total number of cells per visual field (400 μm^2). Cells that were positive for MAP2 or GFAP were scored in 10–15 random nonoverlapping fields in each experiment. The proportion of MAP2- and GFAP-positive cells was expressed as a percentage of the MAP2- and GFAP-positive cells to Hoechst 33382-positive cells, respectively. Each experiment was carried out five times. Figure 3E and 3F show that Stat3 overexpression significantly increased the proportion of the MAP2-positive cells (19.3 ± 1.2% of total cells [mean ± SD] in Ad.LacZ vs. 24.3 ± 1.8% in Ad.Stat3F) and significantly decreased the proportion of GFAP-positive cells (25.7 ± 3.6% in Ad.LacZ vs. 11.4 ± 1.8% in Ad.Stat3F). Taken together, these data suggested that suppression of Stat3 promoted neurogenesis and inhibited astrogliogenesis of neural stem cells.

RT-PCR for Notch Family Members and Inhibitory Basic Helix-Loop-Helix Factors

Based on the Western blot and immunocytochemical results, we examined the effects of Stat3F on the expression of Notch family members or inhibitory basic helix-loop-helix (bHLH) transcription factors that control the fate of neural stem cells. Notch family members and inhibitory bHLH transcription factors play important roles in proliferation, cell lineage determination, and cell differentiation of neural stem cells. We therefore examined the effects of Stat3F overexpression on the mRNA expression of Notch family members (Notch1, 2, and 3) as well as of inhibitory bHLH transcription factors (Hes1, Hes5, Id1, Id2, and Id3) in neural stem cells. Analysis by RT-PCR revealed no changes in the mRNA levels of these genes at 1 day after inoculation (Fig. 4A,B). At 3 days after inoculation, however, the mRNA levels of these genes were decreased by Stat3F overexpression (Fig. 4C,D). The mRNA level of Notch3 was most suppressed by Stat3F (14.4, 19.1, and 42.7% reduction in Notch1, 2, and 3, respectively). Hes5 was more suppressed than Hes1 was (50.4% reduction in Hes5 vs. 16.2% reduction in Hes1). Among the three Id family members, Id3 was most suppressed by Stat3F (7.7, 20.7, and 30.2% reduction in Id1, 2, and 3, respectively). These data suggested that suppression of Stat3 promoted the differentiation of neural stem cells.

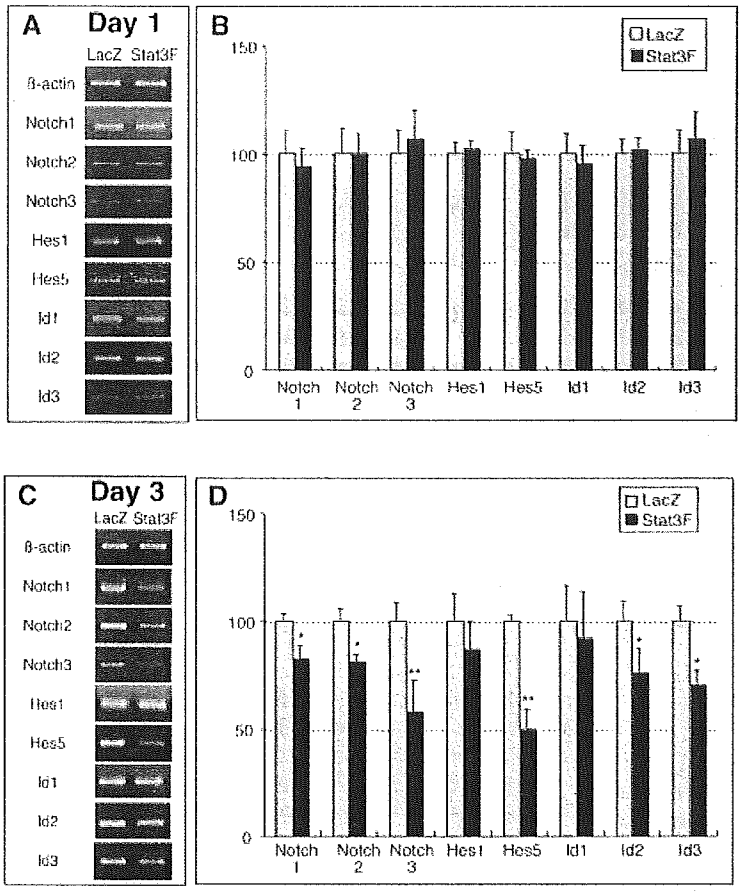

Fig. 4. Effects of dominant negative form of the signal transducer and activator of transcription 3 (Stat3F) on expression of Notch family member and inhibitory basic helix-loop-helix (bHLH) transcription factor mRNA 1 and 3 days after inoculation. RNA was extracted from cells 1 day after inoculation with adenovirus vectors expressing Stat3F or β-galactosidase (LacZ). RT-PCR analyses were conducted to examine mRNA levels of Notch family members (Notch1, 2, and 3) or inhibitory bHLH transcription factors (Hes1, Hes5, Id1, Id2, and Id3). Data were obtained from five independent measurements. Values represent means ± standard deviation. $*P < 0.05$ and $**P < 0.01$, significantly less than LacZ-treated control.

RT-PCR for bHLH Determination and Differentiation Factors

To confirm that Stat3F can induce the neurogenesis in neural stem cells, we examined the effects of Stat3F on the expression of bHLH determination (Mash1, Math1, and Neurogenin3) and bHLH differentiation (NeuroD1 and NeuroD2) factors. The mRNA levels of these transcription factors were not changed at 1 day after inoculation (Fig. 5A,B). At 3 days after inoculation, however, the mRNA levels of the bHLH transcription factors were increased significantly by Stat3F overexpression with the exception of Mash1 mRNA, which remained unchanged (Fig. 5C,D). The average increases in the mRNA levels of these genes were 35.3, 49.5, 43.9, and 39.6% for Math1, Neurogenin3, NeuroD1, and NeuroD2, respectively.

These data also suggested that suppression of Stat3 initiated neurogenesis and promoted terminal neural differentiation of neural stem cells.

DISCUSSION

We demonstrated that suppression of Stat3 promoted neurogenesis and inhibited astrogliogenesis in neural stem cells. These data are in good agreement with several lines of evidence that enhancement of the Janus kinase (Jak)-Stat pathway in neural stem cells leads to subsequent glial differentiation (Bonni et al., 1997; Rajan and McKay, 1998). LIF as well as CNTF and IL-6 can activate the Jak-Stat3 signaling pathway and promote astroglial differentiation (Johe et al., 1996; Bonni et al., 1997). Phosphorylated Stat3 associates with the transcriptional coactivator CREB binding protein (CBP/p300) to activate expression of astrocyte-specific genes (Nakashima et al., 1999). This gliogenic function is suppressed during due to the expression of proneural bHLH factors (such as Neurogenin1). The proneural bHLH factors are highly expressed during neurogenesis. These factors inhibit astroglial differentiation by sequestering Smad1 (vertebrate homologues of Sma and Mad)-CBP/p300 complex away from astrocyte-specific genes and inhibiting activation of Stat3 (Gangemi et al., 2004). DNA methylation of glial genes during the neurogenic period also inhibits glial differentiation by suppressing glial gene transcription and inhibiting Stat3 phosphorylation (Takizawa et al., 2001; Sun et al., 2003). We showed that overexpression of the dominant negative form of Stat3 (Stat3F) suppressed the transcriptional activation of Stat3 and directly inhibited astrogliogenesis in neural stem cells.

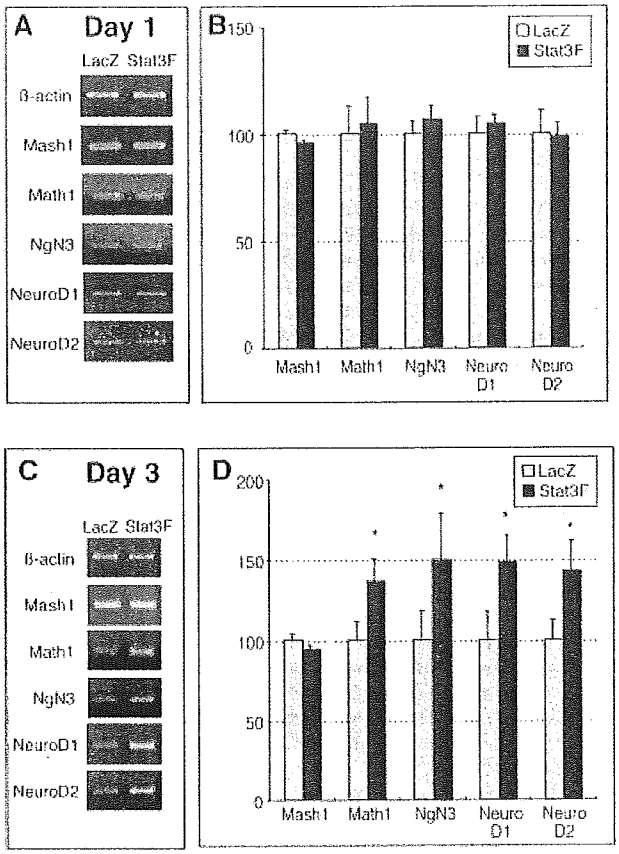

Fig. 5. Effects of dominant negative form of the signal transducer and activator of transcription 3 (Stat3F) treatment on expression of basic helix-loop-helix (bHLH) determination and differentiation factor mRNA 1 and 3 days after inoculation. RNA was extracted from cells 1 day after inoculation with adenovirus vectors expressing Stat3F or β-galactosidase (LacZ). RT-PCR analyses were conducted to examine mRNA levels of bHLH determination factors (Mash1, Math1, and Neurogenin3) or bHLH differentiation factors (NeuroD1 and NeuroD2). Data were obtained from five independent measurements. Values represent means ± standard deviation. $^{*}P < 0.05$, significantly greater than LacZ-treated control.

The present study also demonstrated that Stat3F overexpression significantly reduced mRNA expression of Notch1, 2, and 3 as well as the inhibitory bHLH transcription factors Hes5, Id2, and Id3. During development, Notch signaling plays a widespread role in the assignation of cell fates within the process of lateral inhibition (Iso et al., 2003). Lateral inhibition occurs when cells expressing the Notch ligand contact cells that are expressing Notch. Notch ligand binds and activates Notch on neighboring cells, which causes a reduction in proneural genes in the cells that express Notch. Notch signaling is reported to maintain neural stem cells and inhibit neurogenesis. Hes1 and Hes5 (mammalian hairy and enhancer-of-split homologues 1 and 5) are target genes for Notch signaling. Both Hes1 and Hes5 also maintain neural stem cells in the proliferative state and inhibit neurogenesis (Ohtsuka et al., 2001). Id (inhibitor of DNA binding) proteins negatively regulate bHLH transcription factors that act as transcriptional enhancers or inhibitors of various genes through direct DNA binding to the E-box sequence (Coppe et al., 2003). Although Id proteins contain the HLH domain, enabling them to dimerize with other members of bHLH transcription factors, the resulting Id-bHLH heterodimers cannot bind DNA because Id HLHs lack the basic motif necessary for DNA binding (Benezra et al., 1990). Id proteins are expressed during embryonic development and are important for the regulation of cell phenotypes. In the central nervous system, Id1 and Id3 that have similar expression profiles are typically restricted to the proliferating neuroblasts during the embryonic stage, and increasing evidence points to involvement of these factors in the inhibition of neural differentiation (Tzeng, 2003). Similar to Id1 and Id3, Id2 also functions as an inhibitor of neuronal cell differentiation. Id2 overexpression inhibits the induction of neuron-specific genes and promotes the apoptosis of cortical progenitors (Toma et al., 2000). Furthermore, blockage of Id2 gene expression by Id2 antisense molecules and targeted deletion of the Id2 gene protects neurons from apoptosis (Gleichmann et al., 2002). We demonstrated that inhibition of Stat3 signaling reduces mRNA expression of three members of the Notch family, Hes5, Id2, and Id3. These data suggest that suppression of the Stat3 signaling promotes differentiation of neural stem cells. In fact, it has been reported that Stat3 is activated in the presence of active notch (Kamakura et al., 2004) and that Stat3 signaling is required for the activation of the notch-dependent gene expression (Josten et al., 2004). Our results also provide the lines of evidence that Stat3 and Notch signaling cooperated together in the regulation of the neural stem cell fate.

We also demonstrated that suppression of Stat3 significantly increased the mRNA expressions of bHLH determination or differentiation factors such as Math1, Neurogenin3, NeuroD1, and NeuroD2. The bHLH transcription factors that are involved in vertebrate neurogenesis consist of bHLH determination and differentiation factors, depending on their early or late action during the differentiation process (Lee, 1997). The proteins likely to be bHLH determination factors are Mash1, Math1, and Neurogenins 1–3 (Ngns 1–3), whereas those likely to be bHLH differentiation factors are NeuroD1 and NeuroD2. During brain development, bHLH determination factors are expressed in the ventricular zone where neural stem cells begin differentiation, but not in the cortical plate where fully differentiated neurons are located. Ngns are expressed in the dorsal telencephalon, which gives rise to glutamatergic neurons, whereas Mash1 is expressed predominantly in the ventral telencephalon, which gives rise to γ-aminobutyric acid (GABA)ergic and cholinergic neurons, suggesting that different proneural genes are involved in the specification of different neuronal subtypes (Wilson and Rubenstein, 2000). Math1 is expressed in the neural tube, developing spinal cord, and in the hindbrain, where it

persists in the external granular layer (EGL) of the developing cerebellum (Akazawa et al., 1995). Neural precursors expressing Math1 in the developing spinal cord become dorsal commissural interneurons (Helms and Johnson, 1998) whereas cells that express Math1 in the external granular layer of the developing cerebellum become granule cells (Ben-Arie et al., 1997). In contrast, bHLH differentiation factors such as NeuroD1 and NeuroD2 are expressed in the cortical plate, but not in the ventricular zone (McCormick et al., 1996). In the central nervous system, the NeuroD family is specific to cells that are (or will become) neurons, whereas bHLH determination factors are expressed in neural stem cells that subsequently give rise to both neurons and glial cells. A comparative expression analysis of Ngns and NeuroD has suggested that the former are upstream regulators of NeuroD. The expression of NeuroD seems to follow Ngn expression and NeuroD overexpression does not activate the expression of endogenous Ngn, suggesting that Ngn works as a transcriptional activator of NeuroD (Ma et al., 1996). NeuroD2 seems to be a more downstream regulator of neurogenesis than NeuroD does because of its late onset of expression during embryogenesis and its ability to activate the promoter of more downstream genes, such as GAP-43 (McCormick et al., 1996). Furthermore, whereas ectopic expression of either XNgnr1 or Xash1 results in neuronal differentiation in *Xenopus*, only XNgnr1 mediates the expression of XneuroD and Xath3 (Talikka et al., 2002). Likewise in the mammalian telencephalon, NeuroD1 and NeuroD2 are part of a genetic cascade downstream of Ngns but not of Mash1 (Ross et al., 2003). This might explain why the NeuroD1 and NeuroD2 genes were significantly upregulated after overexpression of the dominant negative form of Stat3 whereas the Mash1 gene was not. Although further investigation is required to clarify this mechanism, our data showed that Stat3 induced upregulation of Math1, Ngn3, NeuroD1, and NeuroD2, leading to the promotion of neurogenesis and their terminal neural differentiation in neural stem cells.

Finally, the immunogenic and cytopathic effects of adenovirus vectors limit their use (St. George, 2003). In fact, exposing neurospheres to recombinant adenovirus vectors has resulted in differentiation into astrocytes, even in the presence of EGF (Hughes et al., 2002). Astrogliogenesis of neurospheres, however, was not apparent after exposure to the virus vector that expressed β-galactosidase at the dosage used in this study (data not shown). Instead, neurogenesis was apparent in the Stat3F-treated group, compared to that in the LacZ-treated group exposed to the same vector titer. Our findings thus were not due to compromising effects of the adenovirus vector.

ACKNOWLEDGMENTS

We thank Dr. K. Ikoma for encouragement and valuable suggestions throughout this work and Ms. K. Hiraoka for secretarial assistance.

REFERENCES

Akazawa C, Ishibashi M, Shimizu C, Nakanishi S, Kageyama R. 1995. A mammalian helix-loop-helix factor structurally related to the product of Drosophila proneural gene atonal is a positive transcriptional regulator expressed in the developing nervous system. J Biol Chem 270:8730–8738.

Alonzi T, Middleton G, Wyatt S, Buchman V, Betz UA, Muller W, Musiani P, Poli V, Davies AM. 2001. Role of STAT3 and PI 3-kinase/Akt in mediating the survival actions of cytokines on sensory neurons. Mol Cell Neurosci 18:270–282.

Ben-Arie N, Bellen HJ, Armstrong DL, McCall AE, Gordadze PR, Guo Q, Matzuk MM, Zoghbi HY. 1997. Math1 is essential for genesis of cerebellar granule neurons. Nature 390:169–172.

Benezra R, Davis RL, Lockshon D, Turner DL, Weintraub H. 1990. The protein Id: a negative regulator of helix-loop-helix DNA binding proteins. Cell 61:49–59.

Bonni A, Sun Y, Nadal-Vicens M, Bhatt A, Frank DA, Rozovsky I, Stahl N, Yancopoulos GD, Greenberg ME. 1997. Regulation of gliogenesis in the central nervous system by the JAK-STAT signaling pathway. Science 278:477–483.

Burdon T, Smith A, Savatier P. 2002. Signalling, cell cycle and pluripotency in embryonic stem cells. Trends Cell Biol 12:432–438.

Coppe JP, Smith AP, Desprez PY. 2003. Id proteins in epithelial cells. Exp Cell Res 285:131–145.

Darnell JE Jr, Kerr IM, Stark GR. 1994. Jak-STAT pathways and transcriptional activation in response to IFNs and other extracellular signaling proteins. Science 264:1415–1421.

Gangemi RM, Perera M, Corte G. 2004. Regulatory genes controlling cell fate choice in embryonic and adult neural stem cells. J Neurochem 89:286–306.

Gleichmann M, Buchheim G, El-Bizri H, Yokota Y, Klockgether T, Kugler S, Bahr M, Weller M, Schulz JB. 2002. Identification of inhibitor-of-differentiation 2 (Id2) as a modulator of neuronal apoptosis. J Neurochem 80:755–762.

Gu F, Hata R, Toku K, Yang L, Ma YJ, Maeda N, Sakanaka M, Tanaka J. 2003. Testosterone up-regulates aquaporin-4 expression in cultured astrocytes. J Neurosci Res 72:709–715.

Heinrich PC, Behrmann I, Muller-Newen G, Schaper F, Graeve L. 1998. Interleukin-6-type cytokine signalling through the gp130/Jak/STAT pathway. Biochem J 334:297–314.

Helms AW, Johnson JE. 1998. Progenitors of dorsal commissural interneurons are defined by MATH1 expression. Development 125:919–928.

Horvath CM. 2000. STAT proteins and transcriptional responses to extracellular signals. Trends Biochem Sci 25:496–502.

Hughes SM, Moussavi-Harami F, Sauter SL, Davidson BL. 2002. Viral-mediated gene transfer to mouse primary neural progenitor cells. Mol Ther 5:16–24.

Iso T, Kedes L, Hamamori Y. 2003. HES and HERP families: multiple effectors of the Notch signaling pathway. J Cell Physiol 194:237–255.

Johe KK, Hazel TG, Muller T, Dugich-Djordjevic MM, McKay RD. 1996. Single factors direct the differentiation of stem cells from the fetal and adult central nervous system. Genes Dev 10:3129–3140.

Josten F, Fuss B, Feix M, Meissner T, Hoch M. 2004. Cooperation of JAK/STAT and Notch signaling in the Drosophila foregut. Dev Biol 267:181–189.

Kamakura S, Oishi K, Yoshimatsu T, Nakafuku M, Masuyama N, Gotoh Y. 2004. Hes binding to STAT3 mediates crosstalk between Notch and JAK-STAT signalling. Nat Cell Biol 6:547–554

Kanegae Y, Makimura M, Saito I. 1994. A simple and efficient method for purification of infectious recombinant adenovirus. Jpn J Med Sci Biol 47:157–166.

Laemmli UK. 1970. Cleavage of structural proteins during the assembly of the head of bacteriophage T4. Nature 227:680–685.

Lee JE. 1997. Basic helix-loop-helix genes in neural development. Curr Opin Neurobiol 7:13–20.

Levy DE, Lee CK. 2002. What does Stat3 do? J Clin Invest 109:1143–1148.

Ma Q, Kintner C, Anderson DJ. 1996. Identification of neurogenin, a vertebrate neuronal determination gene. Cell 87:43–52.

Masumura M, Hata R, Nishimura I, Uetsuki T, Sawada T, Yoshikawa K. 2000. Caspase-3 activation and inflammatory responses in rat hippocampus inoculated with a recombinant adenovirus expressing the Alzheimer amyloid precursor protein. Brain Res Mol Brain Res 80:219–227.

Matsuda T, Nakamura T, Nakao K, Arai T, Katsuki M, Heike T, Yokota T. 1999. STAT3 activation is sufficient to maintain an undifferentiated state of mouse embryonic stem cells. EMBO J 18:4261–4269.

McCormick MB, Tamimi RM, Snider L, Asakura A, Bergstrom D, Tapscott SJ. 1996. NeuroD2 and neuroD3: distinct expression patterns and transcriptional activation potentials within the neuroD gene family. Mol Cell Biol 16:5792–5800.

Molne M, Studer L, Tabar V, Ting YT, Eiden MV, McKay RD. 2000. Early cortical precursors do not undergo LIF-mediated astrocytic differentiation. J Neurosci Res 59:301–311.

Nakajima K, Kusafuka T, Takeda T, Fujitani Y, Nakae K, Hirano T. 1993. Identification of a novel interleukin-6 response element containing an Ets-binding site and a CRE-like site in the junB promoter. Mol Cell Biol 13:3027–3041.

Nakajima K, Yamanaka Y, Nakae K, Kojima H, Ichiba M, Kiuchi N, Kitaoka T, Fukada T, Hibi M, Hirano T. 1996. A central role for Stat3 in IL-6-induced regulation of growth and differentiation in M1 leukemia cells. EMBO J 15:3651–3658.

Nakashima K, Yanagisawa M, Arakawa H, Kimura N, Hisatsune T, Kawabata M, Miyazono K, Taga T. 1999. Synergistic signaling in fetal brain by STAT3-Smad1 complex bridged by p300. Science 284:479–482.

Niwa H, Burdon T, Chambers I, Smith A. 1998. Self-renewal of pluripotent embryonic stem cells is mediated via activation of STAT3. Genes Dev 12:2048–2060.

Ohtsuka T, Sakamoto M, Guillemot F, Kageyama R. 2001. Roles of the basic helix-loop-helix genes Hes1 and Hes5 in expansion of neural stem cells of the developing brain. J Biol Chem 276:30467–30474.

Ozawa Y, Nakao K, Shimazaki T, Takeda J, Akira S, Ishihara K, Hirano T, Oguchi Y, Okano H. 2004. Downregulation of STAT3 activation is required for presumptive rod photoreceptor cells to differentiate in the postnatal retina. Mol Cell Neurosci 26:258–270.

Rajan P, McKay RD. 1998. Multiple routes to astrocytic differentiation in the CNS. J Neurosci 18:3620–3629.

Ross SE, Greenberg ME, Stiles CD. 2003. Basic helix-loop-helix factors in cortical development. Neuron 39:13–25.

St George JA. 2003. Gene therapy progress and prospects: adenoviral vectors. Gene Ther 10:1135–1141.

Sun YE, Martinowich K, Ge W. 2003. Making and repairing the mammalian brain—signaling toward neurogenesis and gliogenesis. Semin Cell Dev Biol 14:161–168.

Takeda K, Noguchi K, Shi W, Tanaka T, Matsumoto M, Yoshida N, Kishimoto T, Akira S. 1997. Targeted disruption of the mouse Stat3 gene leads to early embryonic lethality. Proc Natl Acad Sci USA 94:3801–3804.

Takizawa T, Nakashima K, Namihira M, Ochiai W, Uemura A, Yanagisawa M, Fujita N, Nakao M, Taga T. 2001. DNA methylation is a critical cell-intrinsic determinant of astrocyte differentiation in the fetal brain. Dev Cell 1:749–758.

Talikka M, Perez SE, Zimmerman K. 2002. Distinct patterns of downstream target activation are specified by the helix-loop-helix domain of proneural basic helix-loop-helix transcription factors. Dev Biol 247:137–148.

Toma JG, El-Bizri H, Barnabe-Heider F, Aloyz R, Miller FD. 2000. Evidence that helix-loop-helix proteins collaborate with retinoblastoma tumor suppressor protein to regulate cortical neurogenesis. J Neurosci 20:7648–7656.

Tzeng SF. 2003. Inhibitors of DNA binding in neural cell proliferation and differentiation. Neurochem Res 28:45–52.

Wegenka UM, Buschmann J, Lutticken C, Heinrich PC, Horn F. 1993. Acute-phase response factor, a nuclear factor binding to acute-phase response elements, is rapidly activated by interleukin-6 at the posttranslational level. Mol Cell Biol 13:276–288.

Wilson SW, Rubenstein JL. 2000. Induction and dorsoventral patterning of the telencephalon. Neuron 28:641–651.

Mechanism of Thymus- and Activation-Regulated Chemokine (TARC)/CCL17 Production and its Modulation by Roxithromycin

Mayumi Komine,* Takashi Kakinuma,* Shinji Kagami,* Yasushi Hanakawa,† Koji Hashimoto,† and Kunihiko Tamaki*

*Department of Dermatology, University of Tokyo, Tokyo, Japan; †Department of Dermatology, University of Ehime, Ehime, Japan

Stimulation with tumor necrosis factor (TNF)α and interferon (IFN)γ synergistically induced thymus- and activation-regulated chemokine (TARC)/CCL17 production from HaCaT keratinocytes (KC). Inhibitors for nuclear factor kappa B (NFκB), parthenolide, and Bay 11-7085, and an inhibitor of p38, SB202190, inhibited TNFα- and IFNγ-induced production of CCL17 by HaCaT KC. Surprisingly, an inhibitor of epidermal growth factor receptor tyrosine kinase, PD153035, enhanced the production of CCL17 in HaCaT KC. Roxithromycin (RXM), a 14-membered ring macrolide, suppressed CCL17 production by HaCaT KC induced by IFNγ and TNFα. RXM partially suppressed p38 phosphorylation and NFκB-driven luciferase activity induced by TNFα and IFNγ. Degradation of inhibitor of nuclear factor kappa B (IκB) α upon stimulation with IFNγ and TNFα was not affected by the addition of RXM. Through elucidating the mechanism of CCL17 production, our study indicates that RXM suppresses the production through the inhibition of p38 and NFκB, independent of the inhibition of IκB degradation.

Key words: HaCaT/NFκB/p38/roxithromycin (RXM)/thymus- and activation-regulated chemokine (TARC)/CCL17
J Invest Dermatol 125:491–498, 2005

Thymus- and activation-regulated chemokine (TARC)/CCL17 is a member of the CC chemokine group that is constitutively expressed in the thymus and is produced by monocyte-derived dendritic cells (Imai *et al*, 1996; Zlotnik and Yoshie, 2000) and endothelial cells (Campbell *et al*, 1999). It is a ligand for CC chemokine receptor (CCR) 4 and CCR8 and serves in the recruitment and migration of cells expressing these receptors (Bernardini *et al*, 1998; Sallusto *et al*, 1998). It is considered a Th2-type chemokine because CCR4-expressing T cells mainly produce interleukin (IL)-4. We focused on TARC/CCL17 production from keratinocytes (KC), because TARC/CCL17 has been proven to be essential in skin inflammation (Reiss *et al*, 2001), its existence in the epidermis has been shown (Kakinuma *et al*, 2001), and the serum concentration of TARC/CCL17 is elevated in several inflammatory skin diseases such as atopic dermatitis, and mycosis fungoides (Kakinuma *et al*, 2001, 2003), which suggested to us that TARC/CCL17 produced from KC could be the key molecule in attracting inflammatory lymphocytes to the skin.

Since Kudoh *et al* (1987, 1998) reported their effectiveness in the treatment of diffuse panbronchiolitis (DPB), macrolide antibiotics have been recognized for their anti-inflammatory effects. Macrolides suppress the activity of neutrophils (Oishi *et al*, 1994; Matsuyama *et al*, 1997), production of IL-6 and IL-8 in bronchial epithelial cells (Takizawa *et al*, 1995, 1997), and the function of macrophages (Sugiyama *et al*, 1999). They also inhibit the production of inflammatory cytokines by nasal epithelial cells (Fujita *et al*, 2000). Their clinical effects in patients with dermatological diseases, such as psoriasis (Komine and Tamaki, 2000) and prurigo pigmentosa (Yazawa *et al*, 2001), were also reported. Recently, macrolides have been reported to be effective against bronchial asthma (Shoji *et al*, 1999), acting on eosinophils (Cui *et al*, 2001) and lymphocytes (Noma and Ogawa, 2003), (Noma *et al*, 2001). Roxithromycin (RXM) is one of the newly synthesized 14-membered ring macrolide antibiotics that is effective in treating acne vulgaris and bacterial infections (Bryskier, 1998). It is also effective in treating DPB, and chronic sinusitis, probably due to its anti-inflammatory effects (Scaglione and Rossoni, 1998).

In this study, we first investigated the signaling pathways by which tumor necrosis factor (TNF)α and interferon (IFN)γ stimulate HaCaT KC to produce CCL17, and then tested the ability of RXM to suppress CCL17 production by HaCaT KC. Furthermore, we investigated the inhibitory effect of RXM on various signaling molecules in order to elucidate the mechanism of the suppression of CCL17 production.

Abbreviations: EGFR, epidermal growth factor receptor; IFN, interferon; IκB, inhibitor of nuclear factor kappa B; KC, keratinocyte; MAPK, mitogen-activated protein kinase; NFκB, nuclear factor kappa B; RXM, roxithromycin; (TARC)/CCL17, thymus- and activation-regulated chemokine; TNF, tumor necrosis factor

Results

TNFα and IFNγ synergistically induced TARC/CCL17 production from HaCaT KC Either TNFα or IFNγ alone slightly induced TARC/CCL17 production from HaCaT KC, and the addition of both of these cytokines synergistically induced TARC/CCL17 production (Fig 1). Normal human KC in a monolayer culture did not produce TARC/CCL17 in a

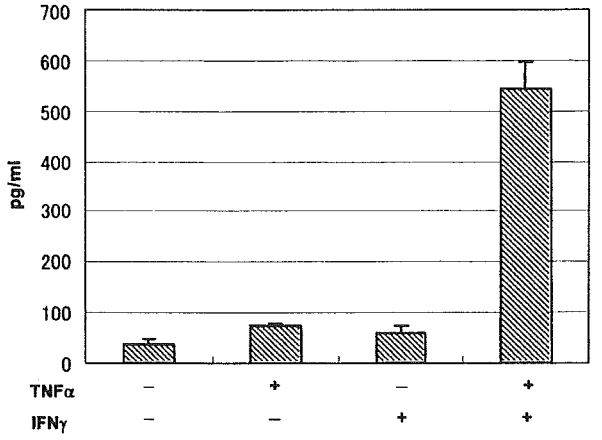

Figure 1
Tumor necrosis factor (TNF)α and interferon (IFN)γ synergistically induce thymus- and activation-regulated chemokine (TARC)/CCL17 production from HaCaT keratinocytes (KC). HaCaT KC were stimulated with TNFα alone, IFNγ alone, or TNFα plus IFNγ, and the concentration of TARC/CCL17 in the supernatant was measured.

similar way, as previously reported (Tsuda *et al*, 2004) (data not shown).

Induction of TARC/CCL17 by TNFα and IFNγ was suppressed by the addition of nuclear factor kappa B (NFκB) inhibitors, Bay 11-7085 and parthenolide, and the p38 inhibitor, SB202190, but not by the extracellular signal-regulated kinase (ERK) inhibitor, PD98059. Addition of the epidermal growth factor receptor (EGFR) tyrosine kinase inhibitor, PD153035, enhanced TARC/CCL17 production We incubated HaCaT KC with the inhibitors of NFκB, p38 mitogen-activated protein kinase (MAPK), ERK MAPK, or EGFR tyrosine kinase for 1 h before stimulation with TNFα and IFNγ. Supernatants were collected and subjected to ELISA. Parthenolide and Bay 11-7085, inhibitors of NFκB activation, and SB202190, the inhibitor of p38 MAPK, strongly inhibited the induction of CCL17 production by TNFα and IFNγ, but PD98059, the inhibitor of ERK MAPK, did not show a significant suppression, which suggests that the induction of CCL17 production by TNFα and IFNγ is dependent on NFκB and p38 MAPK, but not on ERK MAPK. Unexpectedly, the addition of PD153035, the inhibitor of EGFR tyrosine kinase, caused a significant increase in CCL17 production in HaCaT KC, suggesting that the phosphorylation of EGFR has an inhibitory effect on the production of CCL17 by HaCaT KC (Fig 2*a*). These results indicate that either NFκB or p38 is indispensable for TNFα and IFNγ-induced CCL17 production, whereas ERK is not, and that the phosphorylation of EGFR induced by TNFα and IFNγ inhibits CCL17 production. We tried western blotting utilizing the antibody against the phosphorylated tyrosine to observe the tyrosine phosphorylation state of the whole EGFR molecule. Stimulation with TNFα and IFNγ time dependently enhanced the intensity of the EGFR bands that appeared at the molecular weight of 170 kDa, and PD153035 completely abolished these bands (data not shown).

Signal transducer and activator of transcription 1 (STAT1) dominant-negative gene transfer failed to suppress TNFα and IFNγ-induced production of TARC/CCL17 compared with STAT1 wild-type gene-transferred HaCaT cells To investigate the role of STAT1 in the induction of TARC/CCL17 by TNFα and IFNγ, we infected HaCaT KC with an adenovirus vector encoding the STAT1 dominant-negative gene. The blocking of the STAT1 pathway by the STAT1 dominant-negative genes (AxCAdnSTAT1) did not cause any inhibition of TNFα and IFNγ-induced TARC/CCL17 production compared with the induction in cells transferred with STAT1 wild-type genes (AxCAwtSTAT1) (Fig 2*b*). The induction of TARC/CCL17 was weaker when compared with non-transfected cells, probably because of the transfection procedure. This result

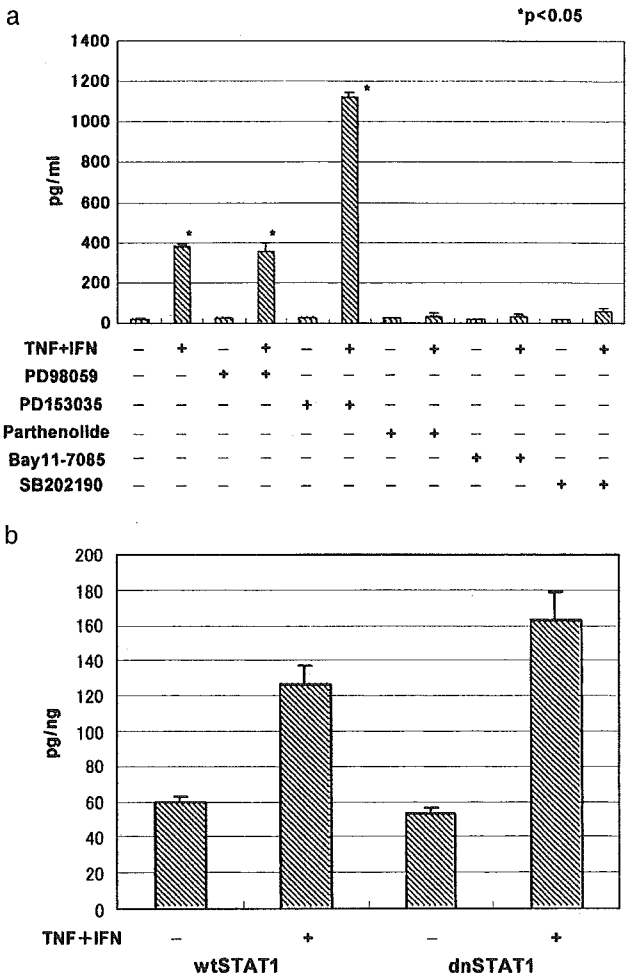

Figure 2
Inhibitors for p38 mitogen-activated protein kinase (MAPK) phosphorylation, and nuclear factor kappa B (NFκB) activation, but not inhibitors for epidermal growth factor receptor tyrosine kinase and ERK MAPK, inhibited thymus- and activation-regulated chemokine (TARC)/CCL17 production by HaCaT keratinocytes (KC). HaCaT KC infected with adenovirus containing STAT1 dominant-negative genes showed similar induction levels of TARC/CCL17 by tumor necrosis factor (TNF)α and interferon (IFN)γ as HaCaT cells infected with adenovirus containing STAT1 wild-type genes. HaCaT KC were incubated with a panel of inhibitors for 1 h before stimulation with TNFα and/or IFNγ. This condition has been previously shown to be effective in suppressing these protein kinases. Supernatants were collected and ELISA was performed (*a*). HaCaT cells were infected with adenovirus containing AxCAwtSTAT1 or AxCAdnSTAT1, starved of serum for 24 h, and stimulated with TNFα and IFNγ. Supernatants were collected after 24 h and subjected to ELISA (*b*).

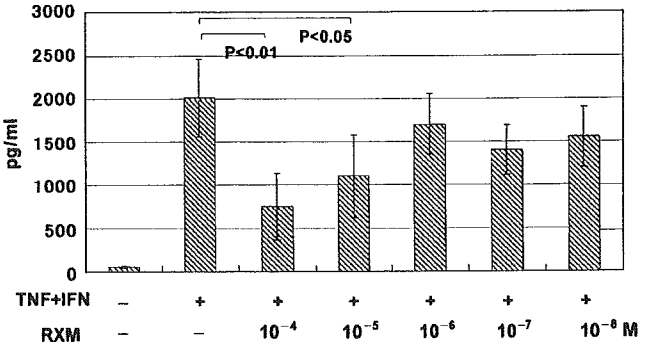

Figure 3
Roxithromycin (RXM) inhibited production of thymus- and activation-regulated chemokine (TARC)/CCL17 by HaCaT keratinocytes (KC) in a concentration-dependent manner. HaCaT KC, starved of FCS for 24 h, were stimulated with tumor necrosis factor (TNF)α (10 ng per mL) and interferon (IFN)γ (10 ng per mL). 10^{-4}, to 10^{-8}, and 10^{-6} M of RXM were added with TNFα and IFNγ. Supernatants were subjected to ELISA.

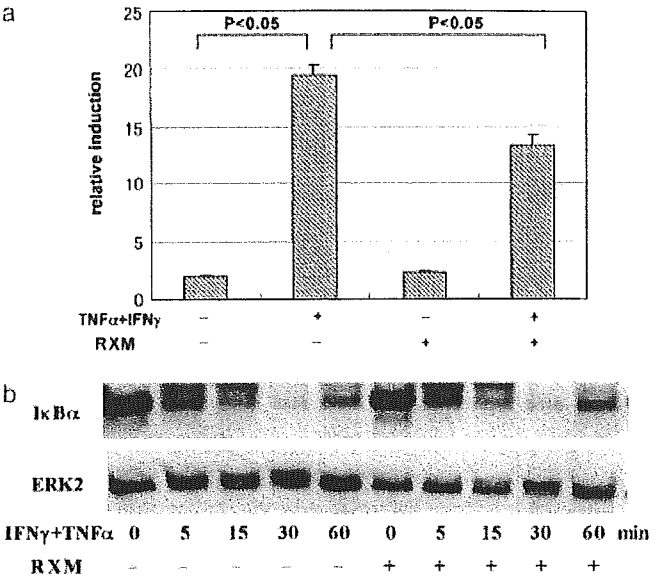

Figure 4
Roxithromycin (RXM) suppressed tumor necrosis factor (TNF)-induced nuclear facor kappa B (NFκB)-driven luciferase activity in HaCaT human keratinocytes (KC). HaCaT KC were grown in minimal essential medium (MEM) with 10% fetal calf serum (FCS) until they became subconfluent. The NFκB-driven luciferase construct and cytomegalovirus (CMV)–renilla luciferase construct were co-transfected into HaCaT KC. RXM was added 2 h before transfection. Both luciferase activities were measured utilizing the dual luciferase assay system. Luciferase activity was normalized against renilla luciferase activity, and the fold induction compared with the non-stimulated condition is shown (*a*). HaCaT KC were starved of FCS for 24 h with or without RXM, stimulated with TNFα and IFNγ, and harvested after the indicated time periods. Cell lysates were subjected to western blotting with the rabbit polyclonal anti-IκBα antibody (*b*). Degradation of inhibitor of nuclear factor kappa B (IκB) induced by TNFα and IFNγ was not affected by the addition of RXM.

indicates that STAT1 activation is not essential in the induction of TARC/CCL17 production by TNFα and IFNγ.

RXM suppressed TARC/CCL17 production induced by TNFα and IFNγ from HaCaT KC Supernatants from cultured HaCaT KC stimulated with TNFα and IFNγ with or without RXM treatment were subjected to ELISA. RXM suppressed the induction of CCL17 production at concentrations of 10^{-4} and 10^{-5} M. The effect was concentration dependent, with almost 80% suppression at 10^{-4} M, and 60% suppression at 10^{-5} M, but was not significant at 10^{-6} M (Fig 3) or lower concentrations.

RXM suppressed NFκB-driven luciferase activity induced by TNFα and IFNγ We assumed that RXM suppresses NFκB transcriptional activation since NFκB was shown to be involved in the induction of CCL17 production by TNFα and IFNγ. We transfected HaCaT KC with an NFκB-driven luciferase construct together with a cytomegalovirus (CMV) renilla luciferase construct. The relative luciferase activity was calculated with CMV renilla luciferase activity as a control. Additions of TNFα and IFNγ caused an almost 9-fold increase in NFκB activity. At 10^{-5} M, RXM significantly suppressed TNFα- and IFNγ-induced NFκB activity in HaCaT KC (Fig 4*a*). These results suggest that the stimulation of HaCaT KC with TNFα and IFNγ leads to NFκB activation, which was essential for CCL17 production. The fact that RXM partially inhibited NFκB activation by TNFα and IFNγ indicated that the suppression of CCL17 by RXM was partially dependent on its NFκB suppression.

We performed a similar experiment in normal human KC in order to confirm the suppression of NFκB activation by RXM, because HaCaT KC have been reported to have abnormal NFκB signaling (Chaturvedi *et al*, 2001). RXM also inhibited the induction of NFκB-driven luciferase activity by TNFα and IFNγ in normal human KC (data not shown).

Inhibitor of nuclear factor kappa B (IκB) is an inhibitory protein that binds to NFκB. Upon stimulation, IκB is phosphorylated and subsequently degraded by the ubiquitin–proteasome pathway. Western blotting with the IκBα antibody revealed that IκBα degradation occurred upon stimulation with TNFα and IFNγ in a time-dependent manner, which was restored after 1 h. This time course of degradation was not affected by the addition of RXM (Fig 4*b*). IκB degradation usually leads to NFκB activation. The fact that RXM did not alter the course of IκB degradation suggests that RXM suppresses NFκB activation independent of IκB degradation, probably at the point after IκB degradation.

RXM suppressed the phosphorylation of p38 and ERK MAP kinases activated by TNFα and IFNγ To investigate whether the phosphorylation of signaling molecules, including p38, is affected by the addition of RXM, western blotting was performed using monoclonal antibodies against phosphorylated forms of these signaling molecules. RXM partially suppressed the phosphorylation of p38 MAPK induced by TNFα and IFNγ (Figs 5*a* and *b*), which showed significant suppression at the 15 and 30 min time points. Phosphorylation of ERK was also slightly suppressed (Figs 5*c* and *d*), which showed significant suppression only at the 5-min time point. But, it did not affect the phosphorylation of c-Jun-N-terminal kinase (JNK) or STAT1 (Fig S1, Fig S2). p38 is crucial for the CCL17 production induced by TNFα and IFNγ as shown in Fig 1, which means that p38 could also be the target of RXM.

We confirmed the suppressive effect of RXM on the phosphorylation of p38 in normal human KC. Normal human KC were incubated in keratinocyte-serum free medium

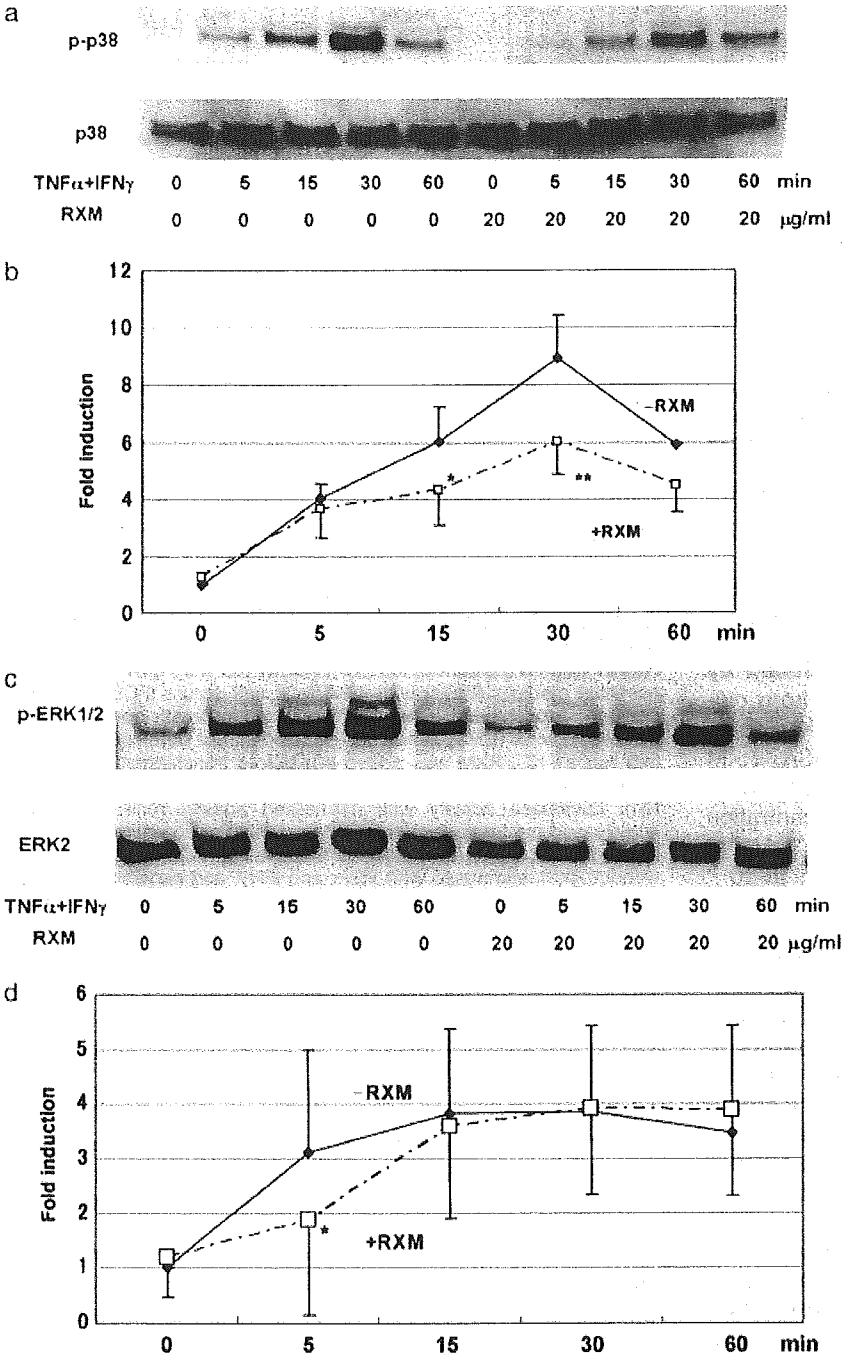

Figure 5
Roxithromycin (RXM) suppressed p38 mitogen-activated protein kinase (MAPK) phosphorylation induced by tumor necrosis factor (TNF)α and interferon (IFN)γ. HaCaT keratinocytes (KC) were starved of fetal calf serum (FCS) for 24 h with or without RXM, stimulated with TNFα and IFNγ, and harvested after the indicated time periods. Cell lysates were subjected to western blotting. Stimulation of HaCaT KC with TNFα and IFNγ caused the phosphorylation of ERK and p38 in a time-dependent manner. Phosphorylation of p38 was attenuated by the addition of RXM (*a*), which showed significant suppression at 30 min when quantified with an image analyzer (*b*). Phosphorylation of ERK was also attenuated by the addition of RXM (*c*), which showed significant suppression at 5 min when quantified with the image analyzer (*d*). Data in the graphs are expressed as the means of triplicates ($^{*}p<0.05$, $^{**}p<0.01$).

(keratinocyte-SFM) without epidermal growth factor (EGF) or bovine pituitary extract (BPE), with or without RXM for 24 h, and then stimulated with TNFα and IFNγ for indicated time periods. The phosphorylation of p38 was suppressed when pre-incubated with RXM; phosphorylations of ERK, JNK, and STAT1 were not affected by the addition of RXM in normal human KC (data not shown).

Discussion

Our result clearly showed that RXM suppressed CCL17 production in HaCaT KC, which is a strong evidence for its action against Th2-type reactions. These findings support its clinical effectiveness against Th2-type inflammations, such as asthma and eosinophilic pustular folliculitis.[1]

TNFα has been reported to cause the activation of various signaling molecules including NFκB (Duh *et al*, 1989), ERK, JNK, and p38 MAP kinases (Kyriaskis *et al*, 1994), and EGFR (Donato *et al*, 1989) in many cell types. In HaCaT KCs, TNFα also activates signaling molecules such as ERK, JNK, and p38 MAP kinases (Holvoet *et al*, 2003), and NFκB

[1]Suzuki S: Personal communication.

(Tomic-Canic *et al*, 1998). IFNγ activates STAT, ERK, and p38 MAP kinases, but not JNK in several cell types (Goh *et al*, 1999), (Nguyen *et al*, 2000). In our experiment, co-stimulation with TNFα and IFNγ of HaCaT KC caused the synergistic upregulation of TARC. It also caused the phosphorylations of ERK, p38 and JNK MAP kinases, the EGFR and STAT1, and degradation of IκB in a time-dependent manner. TNFα alone caused the phosphorylations of ERK, JNK, p38 MAP kinases, and the EGFR, and degradation of IκB, whereas IFNγ alone caused only STAT1 phosphorylation and very weak phosphorylation of p38 within 1 h, among the above molecules investigated (data not shown). The mechanism of synergy is unclear; however, Fujii-Maeda *et al* (2004) recently reported that E-cadherin is essential in the production of TARC/CCL17 in HaCaT KC, whose expression is upregulated by IFNγ and it could be involved in synergistic induction by TNFα and IFNγ. TNFα is also capable of inducing the IFNγ receptor, thereby inducing the synergistic activation of indoleamine deoxygenase by TNFα and IFNγ (Robinson *et al*, 2003). The interaction of signaling molecules, such as STAT1 and NFκB, is also a possible mechanism of synergy, as reported in the transcriptional activation of CXCL9 (Hiroi and Ohmori, 2003); however, dominant negative STAT1-transfected cells showed a response similar to wild-type STAT1-transfected cells, suggesting that STAT1 activation is not essential in the induction of TARC/CCL17 production. Interferon regulatory factors (IRF) are the transcription factors involved in IFNγ signaling, and have been reported to interact with NFκB, which causes the synergistic induction of inducible nitric oxide synthase (Saura *et al*, 1999) and regulated on activation, normal T-cell expressed and secreted (RANTES) (Genin *et al*, 2000). IRF-1, the main IRF family member in IFNγ signaling, however, is induced through STAT1 signaling, which should be STAT1 dependent. Recent investigation revealed that a number of genes are regulated by IFNγ in a STAT1-independent manner. Among them are several chemokines such as macrophage-inflammatory protein-1α and monocyte chemoattractant protein 1 (MCP-1) (Gil *et al*, 2001). Several transcription factors such as EGR-1, C/EBPβ and c-jun are induced in STAT-1 null cells (Ramana *et al*, 2001). Production of TARC by TNFα and IFNγ could be induced through STAT1-independent pathways, the mechanism of which needs further investigation. Recently, Banno *et al* (2003, 2004) reported on a wide spectrum of genes regulated by TNFα or IFNγ utilizing a DNA microarray system. TNFα and IFNγ are pro-inflammatory cytokines involved in innate immunity and inflammation, and the synergistic effect of these cytokines would be a substantial driving force of immunity and inflammation in a biological context. The fact that TARC/CCL17 is only slightly induced by TNFα or IFNγ alone, and strongly induced when they are applied at the same time, suggests that TARC would have a biological meaning, especially when inflammation reaches the level at which both TNFα and IFNγ are abundant, and, at such a level, TARC may have the role of directing the inflammation in a Th2-balanced direction.

The EGFR tyrosine phosphorylation inhibitor enhanced the production of CCL17 stimulated by TNFα and IFNγ. A similar phenomenon has been reported with other chemokines such as CCL2 (MCP-1), CCL5 (RANTES), and CXCL10 (interferon-γ-induced protein of 10 kDa, IP-10) in normal human KC (Mascia *et al*, 2003). EGFR is known to activate various signaling cascades such as ERK, PI3K, and STATs (STAT1, 3, 5). The finding that the EGFR inhibitor enhanced the production of CCL17, whereas the ERK inhibitor had no effect means that the activated EGFR exerts its signal through signaling molecules other than ERK to inhibit CCL17 production. The mechanism of CCL17 production enhancement by the EGFR inhibitor needs further investigation.

Our experiment showed that the mechanisms of CCL17 production in HaCaT and normal human KC are dependent on NFκB activation. This is consistent with a previous report, in which the NFκB inhibitor, MG-132, and mutant IκBα introduced by retroviral vectors inhibited the production of CCL17 in A549 cells, a bronchial epithelial cell line (Berin *et al*, 2001). Our results also indicate that CCL17 production in HaCaT and normal human KC is dependent on p38 MAPK, but not on ERK MAPK, which is also activated in HaCaT KC stimulated by TNFα and IFNγ. A recent study reported on the involvement of p38 and NFκB in CCL17 production in B cells (Nakayama *et al*, 2004), which suggests similar signaling pathways of CCL17 production in B cells and HaCaT KC. Increasing evidence suggests an important role for p38 in adhesion-induced differentiation and signal transduction in epithelial cells. E-cadherin forms adherens junctions in epithelial tissues, providing tight cell–cell contacts. E-cadherin engagement is essential in the activation of p38 in intestinal epithelial cells, which plays a crucial role in intestinal epithelial cell differentiation (Laprise *et al*, 2002). P38 is also involved in the hypotonic stress-induced expression of E-cadherin in HaCaT KC (Kippenberger *et al*, 2005). Taking into consideration the fact that E-cadherin is essential in the spontaneous production of TARC/CCL17 (Fujii-Maeda *et al*, 2004), and that its expression is induced by IFNγ, p38 may be involved in E-cadherin expression induced by IFNγ or in signaling pathways evoked by E-cadherin engagement.

Our results also showed that RXM partially inhibited TNFα- and IFNγ-induced NFκB activation in HaCaT KC, which can explain the inhibitory effect of RXM on CCL17 production in our system. It has been reported that RXM inhibited NFκB activation induced by reactive oxygen intermediates (Abeyama *et al*, 2003) or by Propionibacterium acnes (Chen *et al*, 2002). The inhibition by RXM of NFκB activity induced by TNFα and IFNγ was demonstrated in our experiment.

Erythromycin has been reported to suppress cycloxygenase-2 synthesis in rheumatoid synovial cells by inhibiting p38 activation (Fumimori *et al*, 2004). Clarithromycin suppressed mucin production by inhibiting ERK phosphorylation in the lungs in a murine model of DPB (Kaneko *et al*, 2003). Evidence of RXM inhibiting any of the MAP kinases, however, has not been demonstrated. This report demonstrates that RXM inhibits the phosphorylation of p38 induced by TNFα and IFNγ in KC.

This study, by demonstrating the signaling pathways triggered by TNFα and IFNγ in KC, and the mechanism of RXM action, shed new light on the development of skin